# A Combination Adjuvant for the Induction of Potent Antiviral Immune Responses for a Recombinant SARS-CoV-2 Protein Vaccine

Sonia Jangra[1,3,#], Jeffrey J. Landers[5,6,7#], Raveen Rathnasinghe[1,2,3], Jessica J. O'Konek[5,6,7], Katarzyna W. Janczak[5,6,7], Marilia Cascalho[8,9], Andrew A. Kennedy[5], Andrew W. Tai[5,8,10], James R. Baker, Jr. [5,6,7], Michael Schotsaert[1,3,$], Pamela T. Wong[5,6,7,$]

[1]Department of Microbiology, Icahn School of Medicine at Mount Sinai New York, NY, USA

[2]Graduate School of Biomedical Sciences, Icahn School of Medicine at Mount Sinai, New York, NY, USA

[3]Global Health and Emerging Pathogens Institute, Icahn School of Medicine at Mount Sinai New York, NY, USA

[5]Department of Internal Medicine, University of Michigan Medical School, Ann Arbor, MI, USA

[6]Michigan Nanotechnology Institute for Medicine and Biological Sciences, University of Michigan Medical School, Ann Arbor, MI, USA

[7]Mary H. Weiser Food Allergy Center, University of Michigan Medical School, Ann Arbor, MI, USA

[8]Department of Microbiology and Immunology, University of Michigan

[9]Department of Surgery, University of Michigan Medical School, Ann Arbor, MI, USA

[10]Medicine Service, VA Ann Arbor Healthcare System, Ann Arbor, Michigan, USA

[#]Contributed equally

[$]Corresponding authors:

Michael Schotsaert:Michael.Schotsaert@mssm.edu

Pamela T. Wong: ptw@umich.edu

**Abstract:**

Several promising vaccines for SARS-CoV-2 have received emergency use authorization in various countries and are being administered to the general population. However, many issues associated with the vaccines and the protection they provide remain unresolved, including the duration of conferred immunity, whether or not sterilizing immunity is imparted, and the degree of cross-variant protection that is achieved with these vaccines. Early evidence has suggested potentially reduced vaccine efficacy towards certain viral variants in circulation. Development of

adjuvants compatible with these vaccine platforms that enhance the immune response and guide the adaptive and cellular immune responses towards the types of responses most effective for broad protection against SARS-CoV-2 will likely be pivotal for complete protection. Natural viral infection stimulates strong immune responses through the activation of three main pathways involving Toll-, RIG-I-, and NOD-like receptors (TLRs, RLRs, NLRs). As induction of appropriate innate responses is crucial for long-lasting adaptive immunity and for shaping the correct types of immune responses, we developed a combination, intranasal, adjuvant integrating a nanoemulsion-based adjuvant (NE) that activates TLRs and NLRP3 with an RNA agonist of RIG-I (IVT DI). This rationally designed combination adjuvant yielded a synergistic immune response with highly robust humoral and cellular responses towards SARS-CoV-2 using a recombinant spike protein S1 subunit antigen. Significantly enhanced virus neutralizing antibody titers were achieved towards both a homologous SARS-CoV-2 virus (IC50 titers of $1{:}10^4$) and a mouse-adapted variant containing the N501Y mutation present in the B1.1.7 UK and B.1.351 South Africa variants. Importantly, NE/IVT DI dramatically enhanced the $T_H1$-biased cellular response, which is expected to provide more durable and tailored cellular immunity while avoiding potential vaccine enhanced pathology previously associated with $T_H2$-biased responses in some SARS-CoV and MERS-CoV vaccines. Our previous work with the NE/IVT DI adjuvant has demonstrated its compatibility with a broad range of antigen types. Thus, this combined adjuvant approach has strong potential for improving the induced immune profile for a variety of SARS-CoV-2 vaccine candidates such that better protection against future drift variants and prevention of transmission can be achieved.

## Introduction:

The rapid global spread of severe acute respiratory syndrome coronavirus 2 (SARS-CoV-2) has had a devastating impact on human health and global economies. Global cases of infection have exceeded 100 million, and more than 2.1 million fatalities have resulted[1]. Several promising vaccines including RNA-based, adenovirus vectored, and inactivated viral vaccines are in the final phases of clinical testing and some have now received emergency use authorizations (EUAs) in various countries for administration to the general population[2-4]. Additional candidates including subunit vaccines will soon follow. However, many parameters remain to be determined with these first generation vaccines, such as the duration and breadth of conferred

immunity, whether or not vaccine induced immunity is sterilizing, and real-world efficacy, particularly in cohorts which traditionally display low response rates to vaccination such as the elderly and immunocompromised. In addition, new genetic variants of SARS-CoV-2 have arisen which are reported to show higher transmissibility, increased virulence, and the potential for escape from current vaccines[5, 6]. Thus, it is clear that successful control of the pandemic will require vaccines which can provide not only robust and long-lasting protection, but also confer broad immunity towards these variants and potential future variants yet to emerge. Preliminary studies have already suggested that the potency of neutralizing antibodies induced by the first RNA vaccines may be reduced towards the South Africa B.1.351variant, which contains the N501Y mutation shared by the B.1.1.7 UK variant, and also two other mutations, K417N and E484K, in the spike receptor binding domain (RBD)[7]. We and others have observed that the E484K substitution in the SARS-CoV-2 spike protein receptor binding domain (RBD) can result in reduced neutralization capacity from human convalescent or post-vaccination sera[7-10]. Therefore, high titers of broadly reactive neutralizing antibodies will be important to induce by vaccination in order to provide effective protection against emerging SARS-CoV-2 variants.

Neutralizing antibodies (NAbs) directed towards the SARS-CoV-2 spike protein (S) are an important component of protective immunity conferred by natural infection and vaccines[11-13]. Passive transfer of neutralizing antibodies has been shown to provide protection in non-human primates (NHPs) from high dose viral challenge[14]. However, it is unlikely that antibody responses alone are sufficient for imparting long-lasting and complete protective immunity. Increasing evidence supports an important role of cellular immunity in protection against SARS-CoV-2, especially in preventing severe disease[11, 13]. This is most clearly illustrated by the consistent findings that the presence of NAbs alone does not predict disease severity in COVID-19 patients, with high NAb titers being frequently observed in many cases of severe COVID-19[15]. In contrast, both the presence of SARS-CoV-2 S-specific $CD4^+$ T cells and $CD8^+$ T cells were significantly associated with less severe disease in COVID-19 patients[13]. Furthermore, $CD8^+$ T cell depletion partially abrogated protection from reinfection in NHPs[14]. The importance of both humoral and cellular immunity is not surprising, as these components of the adaptive immune response are highly interdependent. For example, the quality and durability of the neutralizing antibody response as well as B cell memory depend tightly upon $CD4^+$ T cell help,

and $CD4^+$ T cells are involved in a wide spectrum of activities critical to antiviral immunity[16]. Previous studies with SARS-CoV and other respiratory viruses also support the importance of cellular immunity in protection, particularly the essential role of memory $CD8^+$ T cells, especially tissue resident memory T cells ($T_{RM}$'s) in viral clearance[17-20]. Moreover, $CD8^+$ T cells were longer lived in SARS-CoV convalescent patients than $CD4^+$T and B cells and can provide substantial protection in their absence in mouse models[21]. Finally, T cell epitopes are generally more conserved than antibody epitopes as has been observed for other viruses such as influenza virus. Thus, it is clear that a coordinated adaptive immune response composed of robust neutralizing antibodies as well as long-lasting $CD4^+$ and $CD8^+$ T cells are important for complete protection, and will be critical to a successful vaccination strategy.

One strategy for the induction of high levels of neutralizing antibodies and robust protective T cell responses by vaccination is by admixing vaccine antigens with adjuvants. Adjuvants can also promote formation of immune memory, which is important for establishing long-lasting protection, and can help shape immune responses towards those most effective for a particular pathogen. Development of adjuvants compatible with current and future vaccine platforms that enhance the immune response and guide the immune response towards the types of responses that are most effective for protection against SARS-CoV-2 will likely be pivotal for complete protection. Recombinant protein-based SARS-CoV-2 vaccines can especially benefit from adjuvants, as they are poorly immunogenic by themselves. Promising results with adjuvanted recombinant SARS-CoV-2 protein vaccines in clinical trials have been reported[10, 22-24]. Moreover, adjuvants have been used in the past to broaden vaccine responses, such as against antigenically drifted influenza viruses[25, 26], and can also result in antigen dose sparing, a very important feature in the case of a pandemic caused by a newly emerging pathogen like SARS-CoV-2 when vaccines are not available or scarce. Adjuvants work through the induction of innate immune pathways, thereby providing an optimal cytokine and chemokine environment that promotes the induction of quantitatively and qualitatively improved immune responses. For viruses that induce long-lasting immunity, natural viral infection stimulates strong innate immune responses through the activation of three main pathways involving Toll-, RIG-I-, and NOD-like receptors (TLRs, RLRs, NLRs). However, SARS-CoV-2 infection results in a large variability in magnitude of immune responses in recovered patients, with most patients having

relatively stable antibody titers for at least 8 months, but others experiencing rapid waning of antibodies after convalescence[13, 27]. SARS-CoV-2 and –CoV infections induce a muted innate response, with weaker induction of key cytokines and poor activation of type-I interferons (IFN-Is) pathways[28]. IFN-Is are the master activators of the antiviral defense program, and have an essential role in priming adaptive T cell responses and in shaping effector and memory T cell pools[29]. SARS-CoV-2 and –CoV both employ host immunity evasion tactics of inhibiting IFN-I producing pathways at multiple points, including direct inhibition of RIG-I/MAVS as well as inhibiting downstream effector molecules[30]. Furthermore, these viruses have strategies to avoid recognition of their RNA by RLRs[31, 32]. This weak innate response likely contributes to the large variability in magnitude of immune responses in infected patients and duration of protection. TLR signaling also drives T cell responses and promotes affinity maturation of antiviral antibodies. Multivalent stimulation of TLRs through combined agonists enhanced antibody responses in a SARS-CoV vaccine, and skewed responses towards a more $T_H1$ response[33]. As induction of appropriate innate responses is crucial for long-lasting adaptive immunity and for shaping the correct types of immune responses, an adjuvant which can improve activation of these innate pathways would likely lead to enhanced protection in a SARS-CoV-2 vaccine.

Here, we developed a combination mucosal (intranasal) adjuvant integrating a nanoemulsion-based adjuvant (NE) that activates TLRs and NLRP3 with an RNA agonist of RIG-I (IVT DI). This NE formulation has a good safety profile, having established Phase I clinical safety as an intranasal (IN) adjuvant for influenza vaccines, and is currently being tested in another human study[34-36]. NE is an oil-in-water emulsion of soybean oil, a nonionic (Tween80) and cationic (cetylpyridinium chloride) surfactant, and ethanol, developed through screening of a large library of formulations (>200) containing various combinations of surfactants[37, 38]. NE-based immunity is both mucosal and systemic and has a pronounced $T_H1/T_H17$ bias, including an increase in antigen specific $CD4^+$ and $CD8^+$T cells[38-44]. NE activity is mediated at least in part through TLR2 and 4 activation, as well as through induction of immunogenic apoptosis which leads indirectly to NLRP3 activation[39, 44]. NE administered IN imparts robust protective immunity to viruses such as influenza virus, HSV-2, and RSV, without inducing clinical or histopathological signs of immune potentiation. IVT DI is an *in vitro* transcribed RNA consisting of the full-length (546nt) copy-back defective interfering RNA of Sendai virus strain Cantell[45, 46]. The hairpin

structure of IVT DI, along with its dsRNA panhandle and 5' triphosphate, make it a potent and selective RIG-I agonist, and thus, a strong inducer of IFN-Is and ISGs. By combining NE and IVT DI (NE/IVT), ligands for all three pathways (TLR, RLR, and NLR) involved in SARS-CoV-2 innate immunity are provided. Furthermore, the NE also acts as an RNA carrier, facilitating cytosolic delivery of the IVT DI to RIG-I. We have previously demonstrated in an influenza virus model that the combination of these adjuvants synergistically enhanced protective humoral immune responses towards influenza virus when administered IN, which significantly enhanced the antibody response (shortened kinetics, avidity, hemagglutination inhibition, neutralization, subclass profile), and induced a robust antigen specific cellular response with markedly magnified $T_H1$ bias[47]. In these current studies, we immunized animals using this two component adjuvant combined with the recombinant S1 subunit of the SARS-CoV-2 spike protein. The S1 subunit is a target for neutralizing antibodies as it contains the RBD, which binds to the ACE2 receptor on target cells. We demonstrate that adjuvanting S1 with NE/IVT DI, markedly improved the magnitude and quality of the antibody responses towards both the homologous SARS-CoV-2 virus and a divergent mouse-adapted variant containing the N501Y substitution in the spike protein found in the current B.1.1.7 and B.1.351 variants of concern. Passive transfer of the induced antibodies also conferred robust protection against challenge with the heterologous SARS-CoV-2 variant, and resulted in sterilizing immunity. Moreover, robust antigen specific cellular responses with a strong $T_H1$ bias in the presence of a $T_H17$ response was induced with the NE/IVT DI. Both adjuvants are compatible with viral and recombinant protein based antigens and thus provide a flexible platform that can likely improve the immune profile of several current and future vaccine candidates for SARS-CoV-2.

## Materials and Methods:

*Adjuvants and antigen*

NE was produced by emulsification of cetylpyridinium chloride (CPC) and Tween 80 surfactants, ethanol (200 proof), super refined soybean oil (Croda) and purified water using a high speed homogenizer as previously described[38]. CPC and Tween80 were mixed at a 1:6 (w/w) ratio, and homogeneity of particle size ($d$=450-550 nm) and charge (zeta potential=50-55mV) were confirmed. Stability was assessed over several months. Sequence and synthesis methods for

IVT DI RNA have previously been reported in detail[45]. Briefly, SeV DI RNA from SeV-infected A549 cells was amplified using a 5' primer with the T7 promoter and a 3' primer with the hepatitis delta virus genomic ribozyme site followed by the T7 terminator. The resultant DNA was cloned into a pUC19 plasmid and *in vitro* transcribed using a HiScribe T7 High Yield RNA synthesis kit (New England Biolabs). After DNAseI digestion and clean-up with a TURBO DNA-free kit (Thermo-Fisher), IVT DI was purified using an RNeasy purification kit (Qiagen). The absence of endotoxin was verified by limulus amoebocyte lysate assay. Recombinant SARS-CoV-2 spike protein S1 subunit Wuhan-Hu-1 (Val16-Arg685) (accession YP_009724390.1) with a C-terminal His tag was purchased from Sino Biological.

*Cell lines*

Vero E6 cells (ATCC) were maintained in MEM supplemented with 10% heat inactivated (HI) FBS. HEK293T cells expressing human angiotensin-converting enzyme 2 (293T-hACE2) were obtained from BEI resources and maintained in HEK293T medium: DMEM containing 4 mM L-glutamine, 4500 mg/L L-glucose, 1 mM sodium pyruvate and 1500 mg/L sodium bicarbonate, supplemented with 10% heat inactivated fetal bovine serum as previously described[48].

*Viruses*

WT SARS-CoV-2: SARS-CoV-2 clinical isolate USA-WA1/2020 (BEI resources; NR-52281), was propagated by culture in Vero E6 cells as previously described (ref). This isolate is referred to as the WT virus in the current manuscript. MA SARS-CoV-2: Mouse-adapted SARS-CoV-2 was obtained by serial passage of the USA-WA1/2020 clinical isolate in mice of different backgrounds over eleven passages, as well as on mACE2 expressing Vero E6 cells as previously described[49]. Briefly, the virus was passaged every two days via IN inoculation of lung homogenate derived supernatants from infected mice. All viral stocks were analyzed by deep sequencing after propagation to verify the integrity of the original viral genome.

*Lentivirus pseudotyped virus*

Cloning of expression constructs: For generation of spike protein pseudotyped lentivirus (Lenti-CoV2), a codon optimized SARS-CoV-2 spike protein (accession #QHD43416.1) construct was obtained from Sino Biologicals. All cloning was done by the University of Michigan Vector Core. The SARS-CoV-2 spike with 19 amino acids deleted (S□19) was generated by PCR

amplifying the region of spike containing amino acids 738 to 1254 from the full length SARS-CoV-2 spike construct using following primers; Spike BsrGI Gib Fwd 5'-GACCAAGACCTC

TGTGGACTGTACAATGTATATCTGTGGAGAC and Spike Δ19 XbaI Rev 5'-GCCCGAATTCGGCGGCCGCTCTAGAGTTCAACAACAGGAGCCACAGGAAC. The product was cloned into a pCMV3 vector digested at the BsrGI/XhoI sites. Resulting clones were verified by Sanger sequencing. The resulting clone was designated pCMV3-SΔ19. For the generation of a lentiviral vector containing SARS-CoV2–SpikeΔ19, the pCMV3-SΔ19 insert was initially digested with KpnI and blunt polished using Phusion Taq polymerase followed by a DNA cleanup using the Monarch PCR cleanup kit (NEB) and a second digest was done using NotI. The released fragment was then ligated into a pLentiLox-RSV-CMV-Puro vector. Correct insertion was verified by Sanger sequencing. The resulting clone was designated pSARsCoV2delta19AA.

Lenti-CoV-2 pseudovirus expressing the SARS-CoV-2 spike protein was prepared by the University of Michigan Vector Core. Briefly, lentivirus packaging vectors psPAX2 (35 μg), and coronavirus truncated spike envelope pSARsCoV2delta19AA (35 μg) were co-transfected with 70 μg of pGF1-CMV proviral plasmid using standard PEI precipitation methods (ref). PEI precipitation was performed by incubating the plasmids with 420 μg PEI (molecular weight 25,000, Polysciences, Inc) in 10 mL Optimem (Life technologies) at room temp for 20 m, before adding to fresh 90 mL of DMEM media (Life Technologies) supplemented with 10% FBS-1XGlutamax-Pen/Strep 100U/ml. This DNA/PEI containing media was then distributed equally to 5-T150 flasks (Falcon) containing 293T cells. Supernatants were collected and pooled after 72 h, filtered through a 0.45 micron GP Express filter flask (Millipore), pelleted by centrifugation at 13,000 rpms on a Beckman Avanti J-E centrifuge at 4°C for 4 h, and resuspended at 100X the original concentration (~$1\times10^7$ TU/ml) in DMEM (Life technologies). The lentivirus was stored in aliquots at -80 C.

*Animals*

All animal procedures were approved by the Institutional Animal Care and Use Committees (IACUC) at the University of Michigan and Icahn School of Medicine at Mt. Sinai and were carried out in accordance with these guidelines. 6-8-week-old female C57Bl/6 mice (Charles River Laboratories) were housed in specific pathogen-free conditions. Mice were acclimated for

two weeks prior to experiment initiation. For challenge studies, mice were transferred to ABSL3 facilities 2 days prior to serum transfer and subsequent viral challenge.

*Immunization*

For intranasal (IN) immunization, mice were anesthetized under isoflurane using an IMPAC6 precision vaporizer and given 12 µL total (6 µL/nare) of each vaccination mixture. Each group received a total of three immunizations of the same formulations at a 4-week interval. A total of 15 µg of S1 was administered with either PBS, 20% NE (w/v), or 20% NE with 0.5 µg of IVT DI in PBS. Sera were obtained by saphenous vein bleeding 2 and 4 weeks after each immunization, and by cardiac puncture at the end of the experiment at week 10. Bronchial alveolar lavage (BAL) was obtained by gently lavaging lungs with 0.8 ml saline containing protease inhibitors. Spleens and cervical lymph nodes were harvested, processed to single-cell suspensions, and cultured for antigen recall response assessment as previously described[47].

*ELISAs*

Immunograde 96-well ELISA plates (Midsci) were coated with 100 ng of recombinant S1 in 50 µL PBS per well overnight at 4°C. Plates were blocked in 200 µL of 5% non-fat dry milk in PBS for 1 h at 37°C. Serum samples from immunized mice were serially diluted in PBS/0.1% BSA starting at either a dilution of 1:50 or 1:100. Blocking buffer was removed, and diluted sera were added to the wells and incubated for 2h at 37°C followed by overnight incubation at 4°C. Plates were washed three times with PBST (0.05% Tween20), and alkaline phosphatase conjugated secondary antibodies were added (goat-anti-mouse IgG, IgG1, IgG2b, or IgG2c Jackson Immuno Research Laboratories) diluted in PBS/0.1%BSA. Plates were incubated at 37°C for 1h, washed with PBST, and then developed at room temperature by addition of 100 µL of p-nitrophenyl phosphate (pNPP) substrate (Sigma-Aldrich) per well. Absorbance was measured at 405nm on a microplate spectrophotometer. Titers were calculated against naïve sera, using a cutoff value defined by the sum of the average absorbance at the lowest dilution and 2 x standard deviation.

*Pseudovirus microneutralization (MNT) assays*

$9x10^3$ 293T-hACE2 cells were seeded overnight on white clear bottom 96-well tissue culture plates in HEK293T medium. To titer the virus, the lenti-Cov2 stock was serially diluted in HEK293T medium supplemented with 16µg/mL polybrene (Sigma-Aldrich), and incubated for 1h at 37°C to mimic assay conditions for MNT. Diluted virus was then added to the 293T-

hACE2 cells and incubated at 37°C for 4h. The media was removed, and replaced with fresh HEK293T medium without polybrene and incubated for an additional 72h at 37°C. Infection medium was removed and replaced with 20 μL of BrightGlo luminescence reagent using an injection luminometer. Cells were incubated for 2m with shaking and the luminescence was collected over a read time of 1s. For MNT, 293T-hACE2 cells were seeded overnight. Serum samples from immunized mice were serially diluted by a factor of two, starting at a dilution of 1:50 in HEK293T medium supplemented with 16 μg/mL polybrene (Sigma-Aldrich). 50 μL of diluted sera was added to 50 μL of lenti-CoV2-S diluted in the same media to a concentration which gave a luminescence reading of ≥20,000 RLU/well above background in infected cells in the viral titration. Serum and virus were incubated for 1h at 37°C, and then added to 293T-hACE2 cells for incubation at 37°C for 4h. Infection medium was removed, and replaced with fresh HEK293T medium without polybrene and incubated for an additional 72h at 37°C. Luminescence was measured as above. Neutralization titers were determined as the dilution at which the luminescence remained below the luminescence of the (virus only control-uninfected control)/2.

*Microneutralization Assays*

Microneutralization assays with WT SARS-CoV-2 (2019-nCoV/USA-WA1/2020) and the mouse adapted (MA-SARS-CoV-2) variant was performed in a BSL3 facility as previously described (ref). Briefly, 2x104 Vero E6 cells were seeded per well in a 96-well tissue culture plate overnight. Serum samples were heat-inactivated for 30m at 56°C and serially diluted by a factor of 3, starting at dilutions of 1:10 or 1:20 in infection medium (DMEM, 2% FBS, 1x non-essential amino acids). Diluted serum samples were incubated with 450xTCID50 of each virus which (~40 PFU) for 1 hour at 37°C. Growth medium was removed from the Vero E6 cells, and the virus/serum mixture was added to the cells. Plates were incubated at 37°C for 48 h, fixed in 4% formaldehyde, washed with PBS and blocked in PBST (0.1% Tween 20) for 1 h at RT. Cells were permeabilized with 0.1% TritonX100, washed and incubated with anti-SARS-CoV-2-nucleoprotein and anti-SARS-CoV-2-Spike monoclonal antibodies, mixed in 1:1 ratio, for 1.5h at RT. After another wash, cells were incubated with HRP-conjugated goat-anti-mouse IgG secondary antibody for 1h at RT. Cells were washed, and plates were developed by addition of 50 μL tetramethyl benzidine (TMB). Incubation was allowed to proceed until a visible blue color appeared, after which the reaction was quenched by addition of 50 μL 1M $H_2SO_4$. Absorbance

was measured at 450nm and percentage inhibition (reduction of infection) was calculated against the virus only infected control. The 50% inhibitory dilution (IC50) values were calculated for each sample. Undetectable neutralization was designated as a titer of $10^0$. Anti-mouse SARS-CoV-2-nucleoprotein and anti-mouse SARS-CoV-2-spike antibodies were obtained from the Center for Therapeutic Antibody Development at the Icahn School of Medicine at Mount Sinai.

*Antigen Recall Response*

T cell antigen recall response was assessed in cell isolates from the spleen and cervical lymph nodes (cLN) of immunized mice two weeks after the final immunization (week 10). Methods for splenocyte and cLN lymphocyte preparation were previously described (ref). For antigen recall, isolated cells were plated at a density of $8x10^5$cells/well and stimulated with 5 μg per well of recombinant S1 protein in T cell media (DMEM medium with 5% FBS, 2 mM L-glutamine, 1% NEAA, 1 mM sodium pyruvate, 10 mM MOPS, 50 μM 2-mercaptoethanol, 100 IU penicillin, and 100 μg/mL streptomycin), in a total volume of 200 μL per well. Cells were stimulated for 72h at 37°C, and secreted cytokines (IFN-γ, IL-2, IL-4, IL-5, IL-6, IL-17A, TNF-α, and IP-10) were measured relative to unstimulated cells in the cell supernatants using a Milliplex MAP Magnetic Mouse Cytokine/Chemokine Immunoassay.

*Acute cytokine response*

Acute response markers were measured in immunized mice 6 and 12 h post-initial immunization to determine whether the formulations induced reactogenicity. For each group, mice were bled either at 6 or 12 h and the amounts of IFNγ, IL6, IL12p70, and TNFα in the sera were measured using a Procartaplex multiplex immunoassay (ThermoFisher) according to the manufacturer's protocol.

*Passive Transfer and Challenge*

Serum samples were pooled from mice in each immunization group collected after the second boost immunization (wk 10), and 150 μL of the pooled serum was passively transferred into naïve mice through the intraperitoneal route 2h prior to challenge intranasally under mild ketamine/xylazine sedation with $10^4$ PFU of MA-SARS-CoV-2 in 30 μL. Body weight changes were recorded every 24h, and mice were sacrificed at 3 d.p.i. Lungs were harvested and homogenate prepared for virus titration by plaque assay as previously described[49].

*Avidity*

To measure antibody avidity of serum IgG in immunized mice, ELISAs were performed as described above against S1 modified by an additional chaotrope elution step after the overnight incubation of serum on the ELISA plate as previously described[47]. Briefly, after the serum incubation and washes with PBST, 100 µL of PBS, or 0.5 M NaSCN, or 1.5 M NaSCN in PBS at pH 6 was added to each well and incubated at RT for 15 min. The plates were washed three times with PBST, and the ELISA proceeded to development as described above by addition of alkaline phosphatase conjugated goat-anti-mouse IgG.

## Results:

*Safety and acute response evaluation:*

As mentioned above, the NE adjuvant has passed phase I testing in humans as an intranasal (IN) adjuvant and is currently in another ongoing phase I trial. Extensive characterization of this adjuvant has been performed in multiple animal models, each demonstrating optimal safety profiles for use of the adjuvant through both intramuscular and IN routes[43, 50-52]. However, to ensure that simultaneously stimulating TLRs, NLRs, and RIG-I with NE/IVT DI does not lead to over-activation of an inflammatory response, we evaluated the acute cytokine response by assessing the levels of representative cytokines (IL-6, TNF-α, IL12p70, and IFN-γ) in the serum using a multiplex immunoassay at 6 and 12 h post-immunization using a model antigen. We used SARS-CoV-2 RBD as a model antigen. Mice were immunized through the IN route with 10 µg of RBD alone, or combined with the standard doses of NE (20% w/v) or NE/IVT DI (20% NE/0.5 µg IVT DI), used in all subsequent studies discussed below in a total volume of 12 µL PBS per mouse. Minimal or no acute inflammatory cytokines were detectable in the sera at these time points, with only IL-6 being modestly elevated in the NE/RBD (mean 34.4 pg/mL) and NE/IVT DI/RBD (mean 74.7 pg/mL) groups, as compared to the RBD only group (mean 11.6 pg/mL). No significant amounts of TNF-α, IL12p70, and IFN-γ were detectable. These results are consistent with the safety profile of the NE alone, supporting a lack of systemic toxicity with the combined adjuvant. These results are also consistent with the lack of significant changes in body temperature or weight in NE/IVT DI immunized mice in our previous studies with influenza virus antigens (data not shown).

*Characterization of the humoral response induced by immunization with SARS-CoV-2 S1:*

To assess the impact of the combined NE/IVT DI adjuvant on the humoral response, we chose the S1 subunit of the full length SARS-CoV-2 spike protein as the antigen for immunization. We selected the S1 subunit, as it contains the S protein receptor binding domain, which is necessary for forming the interactions with the human ACE2 receptor (hACE2) required for viral entry, and thus contains the key epitopes necessary for neutralizing antibody recognition. Furthermore, previous studies evaluating vaccine candidates for related SARS-CoV have demonstrated that the S1 subunit induces a comparable humoral immune response as the full-length S protein, while avoiding the problems of vaccine associated enhanced respiratory disease (VAERD) and antibody dependent enhancement (ADE) induced by some of the vaccine formulations tested with the native full-length S protein[53]. On the other hand, recombinant SARS-CoV-2 RBD alone was found to be less immunogenic than the S1 and full length S protein by several groups including ours (data not shown and [54, 55]). Moreover, by providing these additional antigenic sites outside of the RBD by immunizing with the S1 subunit rather than the RBD itself, it is possible that improved crossvariant protective immunity can be better achieved. Thus, we selected the S1 subunit for these initial studies. 6-8 wk old C57Bl/6 mice were immunized IN with 15 μg of SARS-CoV-2 S1 alone (S1 only) or with 20% NE (NE/S1), or 20% NE/0.5 μg IVT DI (NE/IVT/S1) according to a prime/boost/boost schedule at a four-week interval. Serum S1-specific total IgG titers were measured two weeks after each immunization (Figure 2). After one immunization, no detectable antigen-specific IgG was observed in the S1 only immunized mice or in the majority of mice immunized with the adjuvants: NE/S1 and NE/IVT/S1 (Figure 2A). However, each adjuvant group had a high responder which displayed detectable S1-specific IgG, displaying a titer of 1:100 for NE/S1, and a titer of 1:6250 for the NE/IVT/S1 group, suggesting the possibility for an improved synergistic effect in early antibody titers with the combined adjuvant upon further optimization of antigen dose. S1-specific IgG increased significantly in both adjuvanted groups after the second immunization, resulting in comparable geomean IgG titers (GMTs) in the range of ~$10^5$ for the NE/S1 and NE/IVT/S1 groups, respectively (Figure 2B), which were further enhanced by the third immunization to titers of ~$10^6$ (Figure 2C). In contrast, the S1 only group showed minimal IgG even after the second immunization, and reached only a mean titer of 1:200 after the third immunization.

As we have previously shown that the combined adjuvant significantly enhances the avidity of antigen-specific IgG from immunized mice to whole influenza virus, we wanted to next examine whether the combined adjuvant also improved the avidity of the induced S1-specific antibodies[47]. Avidity was measured by chaotrope elution of serum S1-specific IgG measured after the second and third immunizations using 0.5 M, and 1.5 M NaSCN in PBS pH 6 (Figure 2D). The NE/S1 and NE/IVT/S1 groups displayed identical antibody avidity for S1 at wk 6, which was significantly enhanced in both groups after the last immunization (wk 10). Both NE and NE/IVT DI induced very high affinity antibodies after three immunizations, with 95-100% of the S1-specific IgG remaining bound even upon elution with a high (1.5M) concentration of NaSCN even at the high dilution of serum tested (1:1,250). Such strong avidity was significantly greater than that of the antibodies evaluated from convalescent COVID-19 patient sera which had only 20-60% of the S1 antibodies remaining bound under a less stringent elution condition of 1 M NaSCN[56].

To examine the IgG subclass distribution induced by the NE and the combined NE/IVT DI adjuvant, the relative titers of IgG1, IgG2b, and IgG2c were measured for the wk 10 sera (Figure 3). Subclass analysis suggests that a balanced $T_H1/T_H2$ profile was elicited for both the NE and NE/IVT DI adjuvants, as has been observed in previous studies with other antigens [42, 47, 57, 58]. Equivalent titers of IgG1 were induced by both NE and NE/IVT DI with GMTs of $5.7x10^5$ and $4.1x10^5$, respectively (Figure 3A). High titers of $T_H1$ associated subclasses were also observed for both the NE and NE/IVT DI. S1-specific IgG2b GMTs of $3.0x10^5$ and $8.2x10^4$ (Figure 3B), and IgG2c GMTs of $3.1x10^4$ and $1.0x10^3$ were observed for NE and NE/IVT DI adjuvanted groups, respectively (Figure 3C). Interestingly, IgG2 subclasses were slightly reduced by the presence of IVT DI in the adjuvant. This is distinct from what was observed in our previous studies using this combined adjuvant with whole inactivated influenza virus as the antigen, in which the presence of IVT DI and other RIG-I activating RNA agonists significantly increased the amount of IgG2 subclasses relative to the NE alone. These results may suggest that these subtle differences are due to the dissimilarities in immunization with a whole inactivated virus containing additional PAMPs, versus the purified recombinant S1 protein. While it is still unclear whether ADCC and ADCP have a prominent role in SARS-CoV-2 immunity, as is the case for influenza virus, the prevalence of antigen specific IgG2b and 2c antibody subclasses is

promising for these other modes of protective immunity outside of antibody neutralization. Importantly, this balanced $T_H1/T_H2$ profile in combination with the cytokine data presented below suggest that these adjuvants avoid the strongly $T_H2$-biased immune responses that have previously been linked to VAERD in SARS-CoV and RSV vaccine candidates adjuvanted with alum.

To examine the functionality of the induced antibodies, viral neutralization was assessed using virus stock prepared from the clinical isolate, 2019-nCoV/USA-WA1/2020, which we classify in this manuscript as "WT" SARS-CoV-2. (Figure 4A, B). The WT SARS-CoV-2 shares a high degree of homology with the Wuhan-Hu-1 isolate from which the S1 subunit used for immunization was derived. To examine the ability of the antibodies from the immunized mice to neutralize a variant with mutations in the S protein, we repeated the neutralization assay with our mouse-adapted SARS-CoV-2 virus (MA-SARS-CoV-2). The MA-virus was generated by serial passaging the WT virus isolate first in the lungs of immune compromised and then in immune competent mice of different backgrounds to optimize mouse virulence, as previously described[49]. As the WT virus is unable to use the endogenously expressed mouse ACE2 receptor (mACE2) for entry, productive infection of the murine respiratory tract is inefficient. Serial passaging allowed for selection of mutations which allowed the virus to adapt to optimally bind and use mACE2 for infection. In the spike protein, the MA-SARS-CoV-2 contains two amino acid mutations compared to the original WT virus from which it was derived, including N501Y and H655Y, and a four amino acid insertion within the S1 subunit as previously described[49]. The N501Y mutation has previously been reported by other groups in an independent mouse adaptation of SARS-CoV-2, and is thus likely to be important for increasing affinity to the mACE2 receptor. Interestingly, the N501Y mutation is shared by both the recently identified circulating variants, B1.1.7 and B.135.1 and is thought to play a role in the increased human to human transmissibility observed for these variants by increasing the affinity of the S protein for the hACE2 receptor. In addition to the changes in the spike protein, the MA-virus also contains three other mutations when compared to the Wuhan-Hu-1 isolate: S194T in the nucleoprotein, T7I in the M protein, and L84S in ORF8. The L84S mutation is however present in the USA-WA1/2020 strain and is most likely not due to mouse adaptation.

As the WT and MA viruses require the use of BSL-3 containment facilities, to facilitate future vaccine candidate screening, a luciferase-based pseudotyped virus assay was validated. A

lentivirus pseudotyped virus expressing the SARS-CoV-2 S protein from the same variant from which the S1 subunit used for immunization was derived (Wuhan-Hu-1), was constructed (Lenti-CoV2), carrying genes for firefly luciferase as described in the methods section. The S protein on Lenti-CoV2 contains aa's 738-1254 of the full length S protein which has a terminal 19 aa deletion which removes an ER retention signal, as it has been shown that this deletion facilitates the generation of spike pseudotyped lentivirus[59].

Microneutralization assays using the WT-SARS-CoV-2 with sera from mice immunized with S1 alone revealed very low or undetectable neutralizing antibody titers, similar to naïve mice after three immunizations (Figure 4A, B). In contrast, mice immunized with NE/S1 showed viral neutralization titers (IC50 GMT 50;range 5-353) after the first boost immunization (wk 6), which was further increased by two orders of magnitude (IC50 GMT $2.6x10^3$;range $0.4\text{-}6.8x10^3$) after the second boost immunization (wk 10). The combined adjuvant enhanced neutralization titers compared to the NE alone. Sera from mice immunized with NE/IVT DI/S1 showed increased IC50 values approximately an order of magnitude higher than the NE/S1 group, giving an IC50 GMT of 340 (range 52 to $3.5x10^3$) and IC50 GMT of $8.6x10^3$ (range $4.3x10^3\text{-}3x10^4$) after the first and second boosts, respectively. Interestingly, this enhancement in virus neutralization was observed with the combined adjuvant, even though there were no differences observed in either the total IgG titers or IgG avidity between the NE/S1 group and the NE/IVT/S1 group at either time point. Notably, the sera from NE/IVT/S1immunized mice after the last immunization reached a maximum of ~100% viral neutralization, and maintained this level of neutralization even down to serum dilutions often reported as the IC50 in a large proportion of human convalescent serum and for antibodies induced by some lead vaccine candidates in humans and in mice[60-62]. While it is difficult to directly extrapolate results, as neutralization assays still need to be standardized for SARS-CoV-2, these results support induction of high-quality antibodies with the combined adjuvant.

Neutralization titers were confirmed using the Lenti-CoV2 pseudotyped virus in a luciferase based assay with 293T-hACE2 cells (Figure 4C). Microneutralization titers (MNTs) determined by measuring reduction in luminescence (viral infection) with the pseudovirus at week 10 showed almost exact correlation with the traditional microneutralization assay with the WT virus. No neutralizing antibodies were detectable with this method for the S1 only group, and a similar degree of enhancement in the MNT (~an order of magnitude increase) was observed for

the combined adjuvant compared to the NE alone, as was seen in the traditional microneutralization assay.

While slightly reduced compared to titers for WT-SARS-CoV-2 and Lenti-CoV2, high cross-variant neutralization titers were still observed when the sera from NE/IVT DI immunized mice were tested against the MA-SARS-CoV-2 (Figure 4D, E). After two immunizations, the difference in enhancement in neutralization by sera from NE/IVT DI immunized mice (IC50 GMT 150; range 34-405) compared to NE alone (IC50 GMT 16;range 2.2-360) appeared to be greater due to the larger drop in the ability of the sera from NE immunized mice to cross-neutralize the MA-virus. However, after the third immunization, differences between the NE and NE/IVT DI groups became similar to the differences observed with the WT virus, as the neutralization titers of both groups increased (IC50 GMT $1.2x10^3$; range 420 to $1.9x10^3$ for NE/S1), (IC50 GMT $1.6x10^3$; range 608 to $3.7x10^3$ for NE/IVT/S1). Thus, this further suggests that the combined adjuvant may strengthen the quality of the antibody response, providing a protective advantage against divergent variants.

*Passive transfer and challenge:*

Neutralizing antibody titers required for protection against SARS-CoV-2 have yet to be determined. However, studies in NHPs suggest that low titers (1:50) administered prior to viral challenge are enough to impart partial protection from a low dose viral challenge, whereas titers of 1:500 conferred full protection to the homologous virus. To determine whether the antibodies raised against the S1 from Wuhan-Hu-1 could protect from heterologous challenge with MA-SARS-CoV-2, week 10 sera from immunized mice were pooled and passively transferred into naïve 6-8 week-old C57Bl/6 mice intraperitoneally before challenging them with $10^4$ PFU virus delivered IN. As previously described, while the MA-virus causes mortality and morbidity in aged mice, young C57Bl/6 mice do not lose body weight in this challenge model, as was the case in this study (Figure 5A). None of the mice receiving serum from immunized animals displayed changes in body weight or increased illness, which also suggests an absence of antibody dependent enhancement (ADE) of disease. Lungs from challenged mice were harvested at 3 d.p.i. for measurement of viral titers in homogenate by plaque assay (Figure 5B). Mice receiving transferred sera from NE/S1 and NE/IVT/S1 groups showed complete sterilizing protection against challenge, with no detectable virus found in the lungs. Given the high neutralizing antibody titers present in both the single and combined adjuvant groups at week 10, it is not

surprising that challenge with this moderate viral dose shows no differences between the groups. In contrast, comparable viral titers were found in mice receiving sera from the S1 only immunized mice as in the group receiving no serum. However, one mouse in the S1 only group controlled infection and showed no viral titers. As previously discussed, this particular MA-virus model represents only mild disease in young mice. Thus, repeating the studies with a high dose viral challenge and with aged mice would likely provide a better distinction between the NE and NE/IVT DI groups.

*Antigen-specific cellular response profile*

Antigen-specific T-cell recall responses were then assessed in splenocytes (Figure 6) and cells isolated from the draining lymph node (cervical lymph node (cLN)) (Figure 7) of the immunized mice two weeks after the last immunization (wk 10). Splenocytes and cLN were stimulated with recombinant S1 for 72 h, and cytokine secretion was measured in the cell supernatant by multiplex immunoassay. NE/IVT DI administered through the IN route with S1, induced a heavily magnified $T_H1$ biased response particularly in the draining LN as compared to the NE/S1 single adjuvant group. IFN-γ production in the NE/IVT DI group was increased by an average of 6-fold and by as high as 60-fold, in the spleen, and increased an average of 10-fold and by as high as 230-fold in the cLN as compared to the NE group (Figures 6A, 7A). IL-2 production in the NE/IVT DI group was also increased by an average of 2-fold and by as high as 8-fold in the spleen, and increased by an average of 5-fold and by as high as 28-fold in the cLN as compared to the NE group. Additionally, IP-10 and TNF-α were both also enhanced in the spleen and cLN as compared to the NE group. This magnification of $T_H1$ associated cytokines and TNF-α is significant, as co-production of IFN-γ, IL-2, and TNF-α on polyfunctional antigen-specific T-cells has been shown to be the single strongest criteria for predicting vaccine-elicited T-cell mediated protection against viral infection[63, 64]. Upon analysis of $T_H2$ associated cytokines, no significant IL-4 induction was observed in any of the treatment groups, and only minimal levels of IL-13 were observed with NE or NE/IVT DI that were equivalent to that induced by the antigen alone (Figure 6G,I, 7G,I). NE/IVT DI immunized mice showed slightly higher levels of IL-5 in splenocytes compared to NE alone, however, levels of IL-5 were low overall, being well below that induced by the S1 alone (Figure 6H). In fact, immunization with NE or NE/IVT DI appeared to reduce the amount of IL-5 and IL-13 induced by the S1 alone. and (ex. NE/IVT DI IL-5 was ~5-10-fold lower than the S1 only group). While IL-5 levels were higher in the cLN, a

similar pattern applied in which NE and NE/IVT DI had similar or reduced levels of IL-5 relative to the S1 alone (Figure 7H). Interestingly, when we compared IL-5 production after immunization through the IM route with Addavax (MF59), markedly higher levels of IL-5 (>3,000 pg/mL) were produced in the spleen and cLN upon antigen recall evaluation than the NE or NE/IVT groups (Figure S1).

In addition to the $T_H1$ response, a pronounced $T_H17$ response as indicated by the production of IL-17A was also induced by the NE and enhanced significantly by the NE/IVT DI in the spleen and the cLN. NE/IVT DI enhanced IL-17A production by an average of ~10-fold in the spleen, and ~7-fold in the cLN relative to the NE group. We have previously observed a similar cytokine response profile including magnified $T_H1$ and $T_H17$ responses upon immunization of mice with NE/IVT DI and inactivated influenza virus. Induction of a $T_H17$ response is unique to the mucosal route of immunization with NE, and we have previously demonstrated that it is a critical component of NE-mediated protective immunity through the IN route.

**Discussion:**

In this work we show the potency of adjuvants for the induction of safe protective immune responses against SARS-CoV-2 by vaccination via the intranasal route. As vaccine antigen we used recombinantly produced S1 subunit of the SARS-CoV-2 spike protein. Recombinant protein-based vaccines are able to hone immune responses towards specific, well-defined neutralizing epitopes, and production is readily scalable. However, subunit vaccines are less immunogenic than whole virus antigens and viral vectored vaccines, requiring adjuvants to optimize immunogenicity. We indeed observed that vaccination with S1 in the absence of adjuvant did not result in potent vaccine responses. Previously, we described the use and safety profile of NE and the advantages of the combination of NE/IVT DI for influenza virus vaccines[47]. In this study, we demonstrate that our combined adjuvant approach results in optimal vaccine responses consisting of high avidity antibodies and high neutralization titers measured with both a luciferase-based pseudotyped virus assay and a standard microneutralization assay with the WT virus. Both pseudovirus- and WT virus-based microneutralization assays showed a strong correlation, which is in line with previous reports. Furthermore, the combined adjuvant induced antibodies which better maintained neutralizing capabilities towards a heterologous mouse-adapted SARS-CoV-2. Our data show that high microneutralization titers obtained after

three immunizations can result in sterilizing immunity to a heterologous variant containing the N501Y mutation when antibodies are transferred into naïve animals before viral challenge. As the amount of serum used for transfer was small (150 μl), it is likely that the amount of vaccinations to induce sterilizing immunity can be reduced to two or even a single vaccination, as we have reported for intramuscular SARS-CoV-2 vaccination in mice with a TLR7/8 agonist as adjuvant using a slightly different SARS-CoV-2 challenge model[65]. The outcome of current clinical trials with adjuvanted recombinant protein vaccines for COVID-19 will guide further optimization of dose and formulation.

We show that by better activating TLRs, NLRs, and RIG-I with the NE/IVT DI, cellular immunity could also be enhanced, skewing responses towards a strong $T_H1$ bias, with magnified IFN-γ, and increased IL-2, IP-10 and TNF-α production upon antigen recall in the spleen and draining lymph nodes. In contrast, $T_H2$ associated cytokines, IL-4, IL-5, and IL-13 were not increased compared to the S1 alone immunized group. VAERD was previously reported for certain SARS-CoV vaccine candidates, and has been primarily attributed to poor antibody quality in the context of adjuvant (alum) enhanced $T_H2$ immunopathology. In these cases, accentuated production of IL-4, IL-5, and IL-13 upon viral exposure in vaccinated animals resulted in increased recruitment of eosinophils to the lung, leading to potentiation of airway inflammation, hyperresponsiveness, and lung dysfunction, particularly in aged animals[66, 67]. Our combined adjuvant approach results in a cytokine environment that heavily favors the induction of type 1 immune responses with potent T cell activation along with high quality antibody responses, which provides an optimal immune response profile for avoiding VAERD and ADE upon virus encounter.

We have previously demonstrated that induction of a $T_H17$ response is unique to the mucosal route of immunization with NE, and that it is a critical component of NE-mediated protective immunity. While the role of the $T_H17$ response in SARS-CoV-2 immunity remains to be determined, a robust $T_H17$ response is important for promoting effective immunity to several respiratory viruses, including influenza virus, in which it is associated with enhanced viral clearance and survival[68, 69]. In addition, $T_H17$ lineage $CD4^+$ T cells play a critical role in effective mucosal immunity and the development of $T_{RM}$'s in the lung, which increasing evidence supports, are critical elements of immunity to SARS-CoV-2[70]. Indeed, both NE and NE/IVT DI

adjuvants induced S1-specific IgA in the bronchial alveolar lavage fluid (BAL) (Figure S2). Induction of $T_H17$ responses have been associated with detrimental pathology in certain situations, including autoimmunity, however this is highly dependent on the cytokine milieu in which the response is induced. IL-17A associated pathology in the lung primarily has been observed in the context of high $T_H2$ cytokines, whereas pathological inflammatory effects of IL-17A are prevented by IL10[71]. While IL10 was not measured in the current study, our previous work with influenza virus antigens and SARS-CoV-2 RBD have demonstrated significant enhancement of IL10 with the NE/IVT DI adjuvant[47]. The NE and NE/IVT DI do not induce high levels of $T_H2$ cytokines, while enhancing $T_H1$ cytokines and IL-10, and thus, we believe that this profile of T-cell activation will lead to significantly enhanced viral clearance without detrimental inflammation, as we have observed in our prior studies with NE and NE/IVT DI with influenza virus challenge. Furthermore, IL-17A induced by IN NE vaccination improves protective efficacy to RSV without increased lung pathology or eosinophilia upon challenge in mouse and cotton rat models[72]. While IL-17A is strongly upregulated in COVID-19 patients during cytokine storm, it is likely that inducing IL-17A early, and in the context of an appropriate cytokine milieu (without strongly $T_H2$ responses), will be important for driving protective immunity rather than pathology. Mucosal immunity plays an important role in immunity to most respiratory viruses and can prevent viral transmission. Moreover, induction of effective mucosal responses can prevent viral dissemination to the lung, and $CD8^+$ $T_{RM}$'s residing in the lung mucosa can act early before circulating effector memory and central memory cells can be recruited[73]. Thus, inducing a safe and effective $T_H17$ response through mucosal vaccination can likely better provide these components of immunity than parenteral vaccines. However, much remains to be determined regarding the mucosal immune responses to SARS-CoV-2, and further studies are required.

The COVID-19 pandemic is a quickly evolving landscape, and much is still being learned regarding the correlates of protection to SARS-CoV-2. There is broad consensus that NAbs are critical for protection, however it is becoming clear that antibody responses alone will not be sufficient for full and long-lasting immunity. We have learned from SARS-CoV and now – CoV2, that T cell responses are important for preventing severe disease and for promoting long-term immunity. Together, our data demonstrate that combination of NE/IVT DI offers a promising strategy for promoting both robust antibody and T cell responses to improve

protection against SARS-CoV-2. Importantly the robust neutralizing antibody response induced by NE/IVT DI provides sterilizing cross-protective immunity which will likely be further strengthened in the context of the strong T cell responses induced. Thus, this adjuvant has the potential to also improve the breadth of induced immunity against future drift variants. Furthermore, the ability to use NE/IVT DI through the IN route offers the added advantage of inducing these antiviral immune responses via the respiratory tract, the natural route of viral entry, which promotes improved mucosal immunity. Intranasal administration also offers logistical advantages such as the ease of needle-free administration, which is important for mass vaccination campaigns, especially in resource-poor areas. As NE/IVT DI is compatible with both whole viral antigens and recombinant antigens, it thus provides a flexible platform that has the potential to improve the immune profiles of multiple vaccine candidates currently in development for SARS-CoV-2.

**Acknowledgements:**

We thank the U of M vector core and Dr. Tom Lanigan for producing the lentivirus pseudovirus and for providing technical input on assays. The authors gratefully thank Adolfo García-Sastre and Raffael Nachbagauer at the Icahn School of Medicine at Mount Sinai, New York, NY for support, use of laboratory infrastructure and helpful discussions. We also thank Richard Cadagan for excellent technical assistance and Randy Albrecht for BSL3 support. This research was partly funded by CRIP (Center for Research for Influenza Pathogenesis), a NIAID supported Center of Excellence for Influenza Research and Surveillance (CEIRS, contract # HHSN272201400008C), by supplements to NIAID grant U01AI124297 and by Collaborative Influenza Vaccine Innovation Centers (CIVIC) contract 75N93019C00051.

**Figure 1.** Acute cytokine response was assessed in the serum by measuring (A) IL-6, (B) TNF-α, (C) IL12p70, and (D) IFN-γ by multiplex immunoassay at 6 and 12 h post-IN immunization with 10 μg of RBD only, or with 20% NE, or 20% NE/0.5 μg IVT DI.

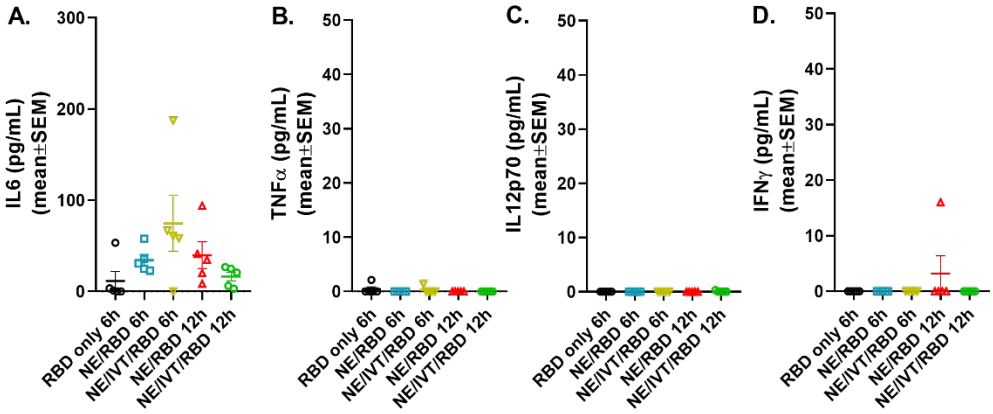

**Figure 2.** Serum S1-specific IgG measured in mice immunized IN with 15 µg S1 alone, or with 20% NE, or 20%/0.5 µg IVT DI. S1-specific IgG was measured 2 weeks after each immunization at (A) 2 wks post-initial immunization (prime), (B) 6 wks post-initial immunization (prime/boost), and (C) 10 wks post-initial immunization (prime/boost/boost). (*p<0.05, **p<0.01 by Mann-Whitney U test). (D) Antibody avidity for S1-specific IgG measured by NaSCN elution for a 1:1,250 dilution of serum for the 6 wk and 10 wk sera. The control group (ctrl) consisted of untreated mice.

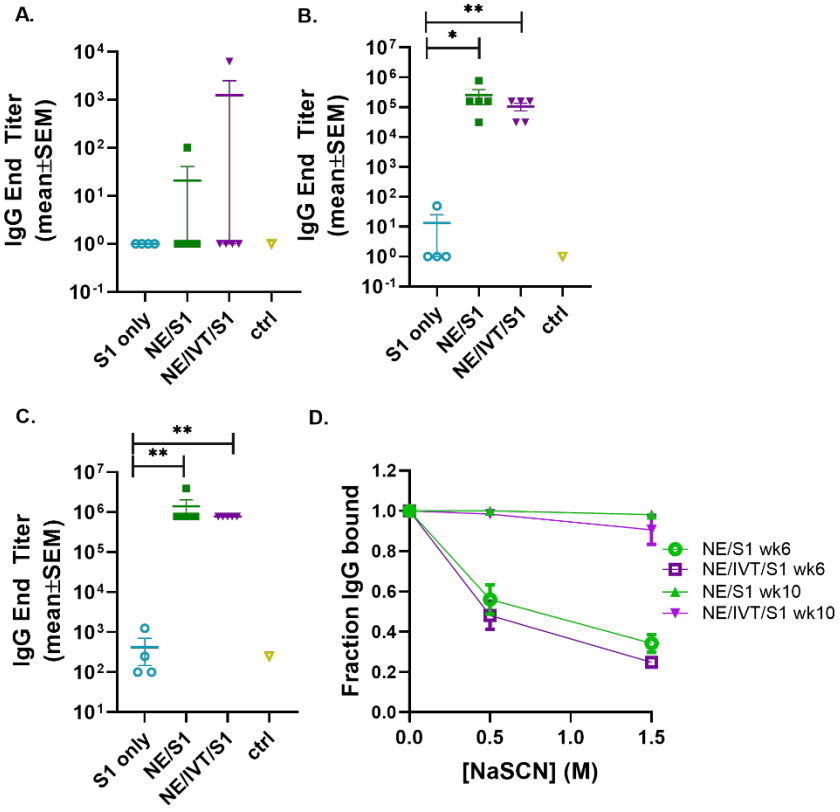

**Figure 3.** Serum S1-specific IgG subclasses (A) IgG1, (B) IgG2b, and (C) IgG2c were measured in mice immunized IN with 15 µg S1 alone, or with 20% NE, or 20%/0.5 µg IVT DI after the last boost immunization, 10 wks post-initial immunization. (*p<0.05, **p<0.01 by Mann-Whitney U test).

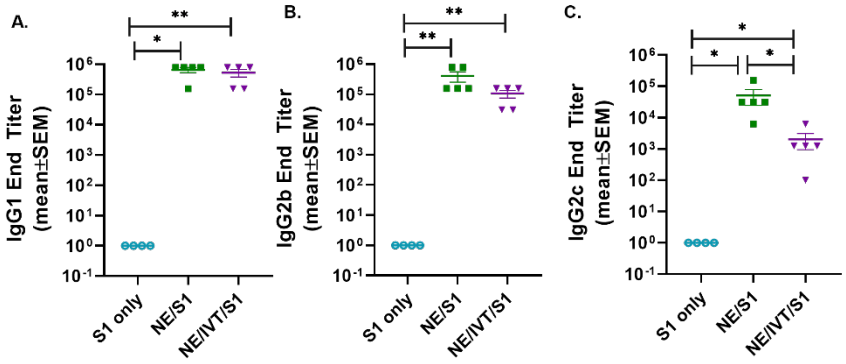

**Figure 4.** Neutralizing antibody titers in serum from mice receiving two (wk 6) or three (wk 10) immunizations mice were determined using microneutralization assays against the WT SARS-CoV-2 (2019-nCoV/USA-WA1/2020), pseudotyped lentivirus expressing the WT SARS-CoV-2 spike protein (Lenti-CoV2), and MA SARS-CoV-2. Viral neutralization was plotted as percentage inhibition of viral infection in Vero E6 cells (for WT virus and MA-virus) relative to virus only (no serum) positive controls versus the inverse serum dilution. The titer at which 50% inhibition of infection was achieved (IC50) was determined for the (A, B) WT virus and the (D, E) MA virus. (C) The results were confirmed for the same week 10 serum samples using the Lenti-CoV2 pseudovirus expressing firefly luciferase with HEK-293T cells expressing hACE2. Microneutralization titers using the Lenti-CoV2 were determined by detecting viral infection by measuring luminescence (*p<0.05, **p<0.01 by Mann-Whitney U test). Pretreatment (pre) sera were obtained from the same set of mice before immunizations.

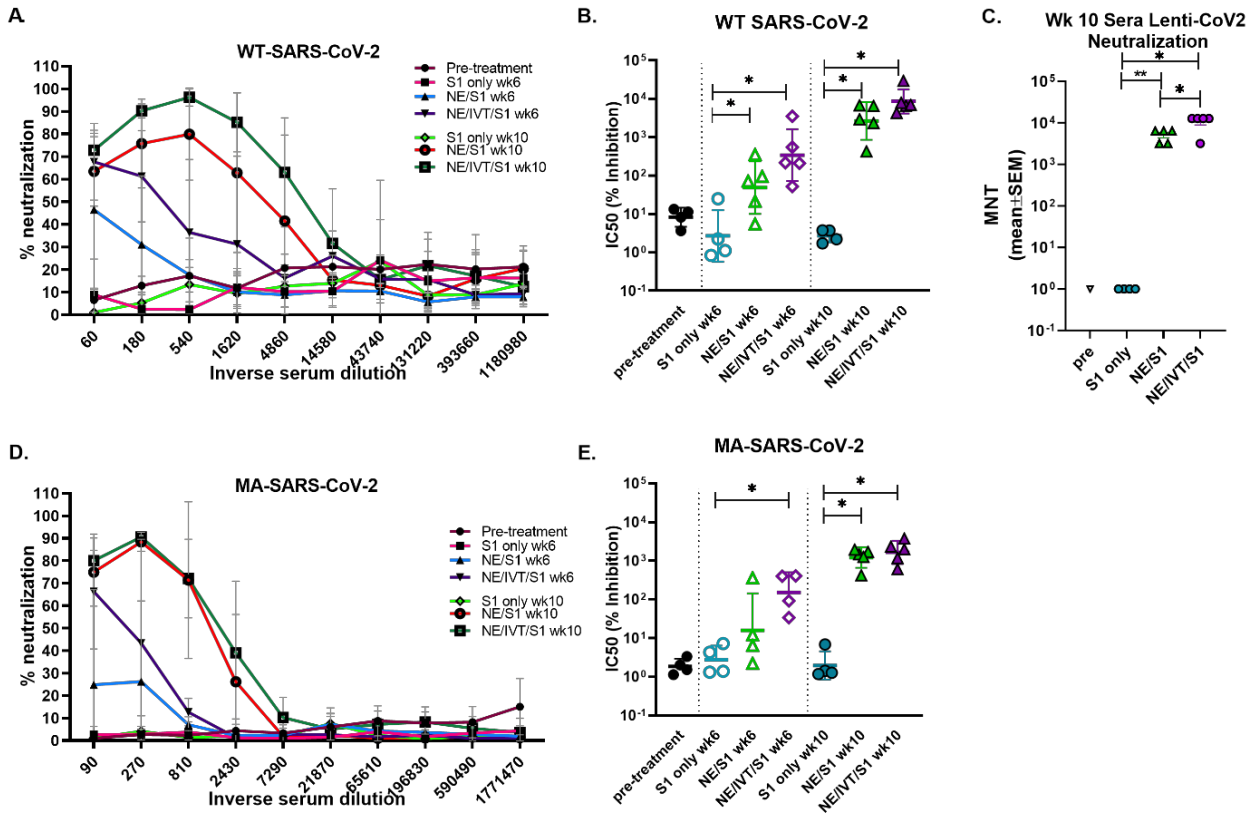

**Figure 5.** Passive serum transfer. Naïve C57Bl/6 mice (n=3-4/group) each received 150 µL of pooled serum through the intraperitoneal route from donor mice given three IN immunizations of S1, NE/S1, or NE/IVT/S1. 2 h after serum transfer, mice were challenged IN with $10^4$ PFU of MA-SARS-CoV-2. (A) Body weight loss was measured over three days, and at 3 dpi (B) lung virus titers were determined in homogenate by plaque assay. (*p<0.05, **p<0.01 by Mann-Whitney U test)

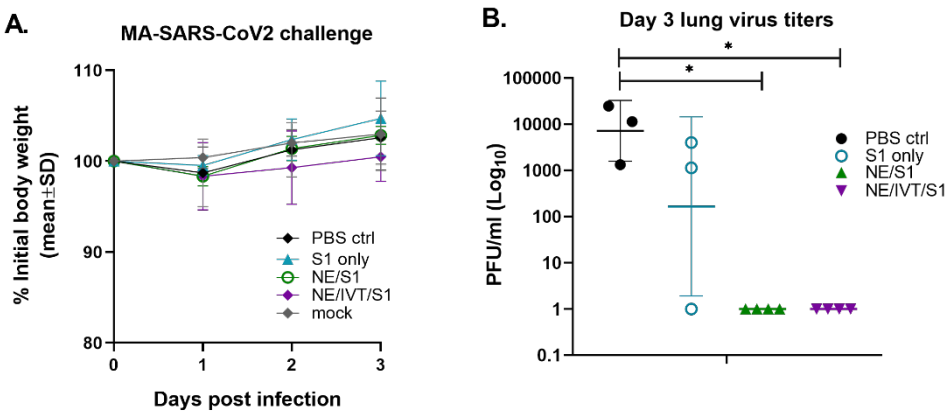

**Figure 6:** Antigen recall response assessed in splenocytes isolated from mice immunized IN with S1 alone, or with NE, or NE/IVT DI after the final boost immunization (10 weeks post-initial immunization). Splenocytes were stimulated ex vivo with 5 μg of recombinant S1 for 72h, and levels of secreted cytokines (A) IFNγ, (B) IL2, (C) IP10, (D) TNFα, (E) IL6, (F) IL17A, (G) IL4, (H) IL5, (I) IL13 were measured in the supernatant relative to unstimulated cells by multiplex immunoassay. An unvaccinated control was included for comparison. (*n*=5/grp; *p<0.05, **p<0.01 by Mann-Whitney U test)

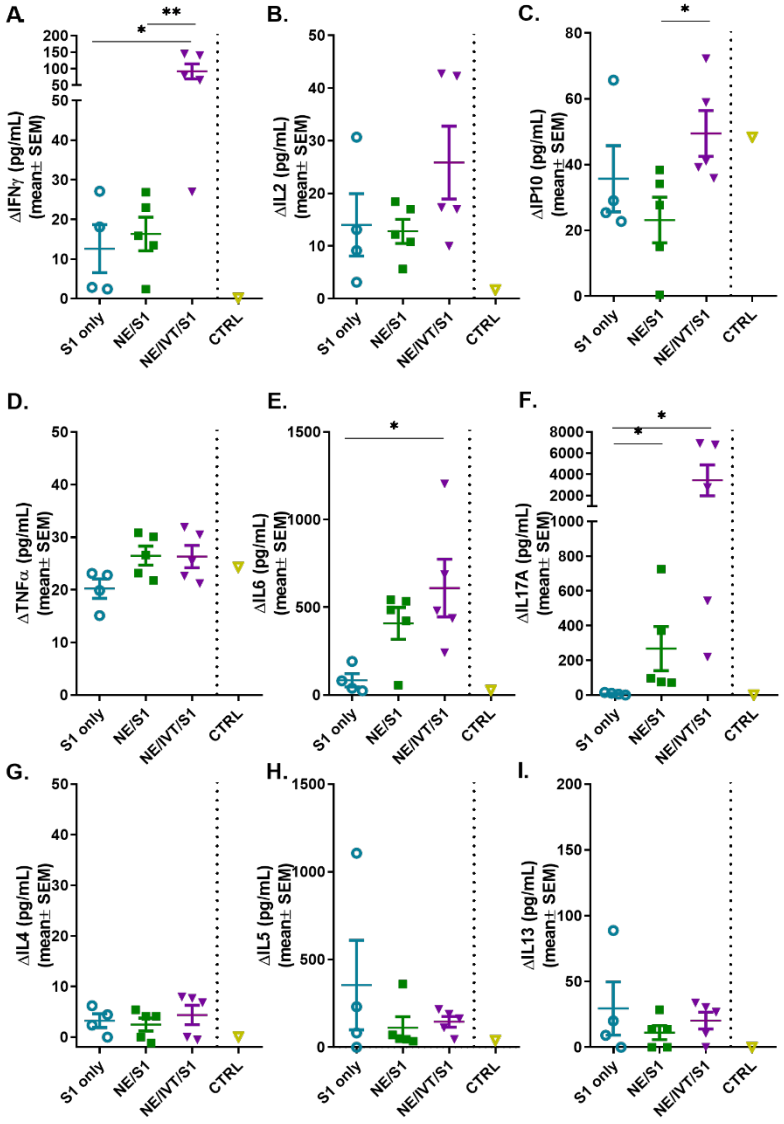

**Figure 7:** Antigen recall response assessed in lymphocytes from draining lymph nodes (cLN) isolated from mice immunized IN with S1 alone, or with NE, or NE/IVT DI after the final boost immunization (10 weeks post-initial immunization). Cells were stimulated *ex vivo* with 5 μg of recombinant S1 for 72h, and levels of secreted cytokines (A) IFNγ, (B) IL2, (C) IP10, (D) TNFα, (E) IL6, (F) IL17A, (G) IL4, (H) IL5, (I) IL13 were measured in the supernatant relative to unstimulated cells by multiplex immunoassay. An unvaccinated control was included for comparison. ($n$=5/grp; *p<0.05, **p<0.01 by Mann-Whitney U test)

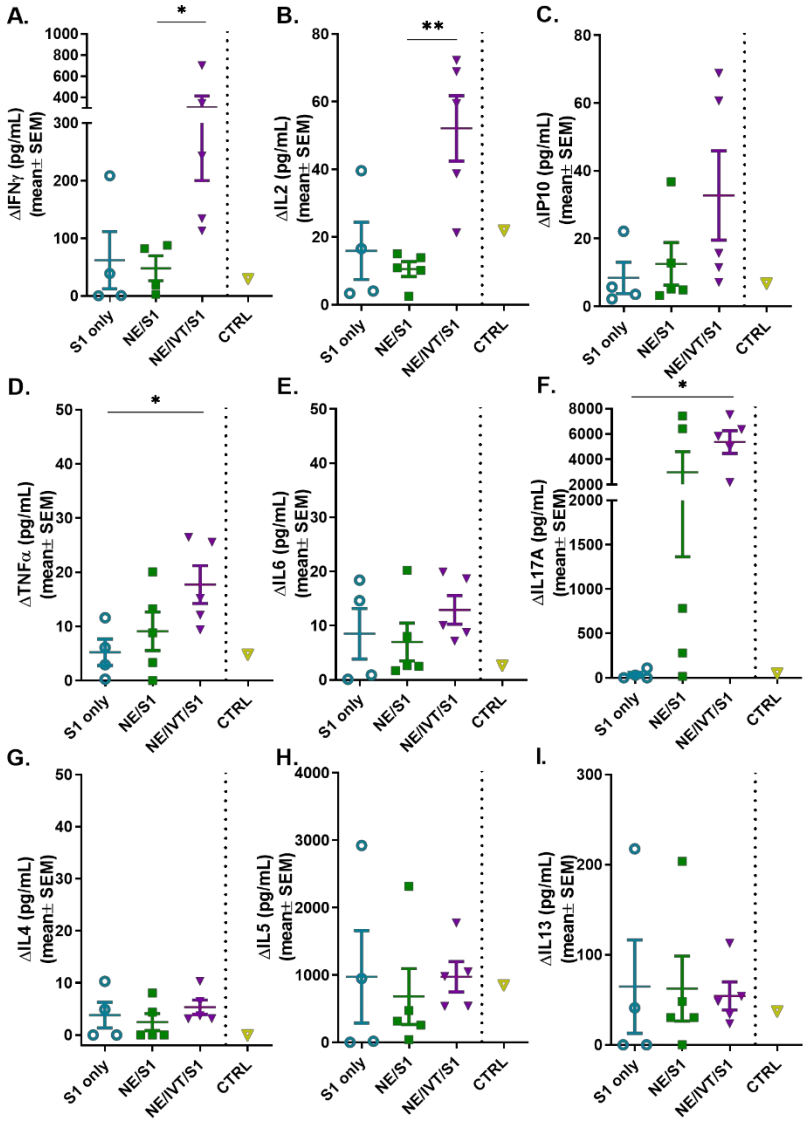

## Supplemental Information:

**Supplemental Figure S1:** Antigen recall response assessed in lymphocytes from spleen and cLN isolated from mice immunized IM with 10 µg SARS-CoV-2 RBD alone, or with 50% Addavax NE in a volume of 50 µL according to a prime/boost/boost schedule (at a 4 wk interval). Cells were stimulated *ex vivo* with 5 µg of recombinant RBD for 72h, and levels of secreted IL-5 were measured in the supernatant relative to unstimulated cells by multiplex immunoassay. (*n*=5/grp; *p<0.05, **p<0.01 by Mann-Whitney U test)

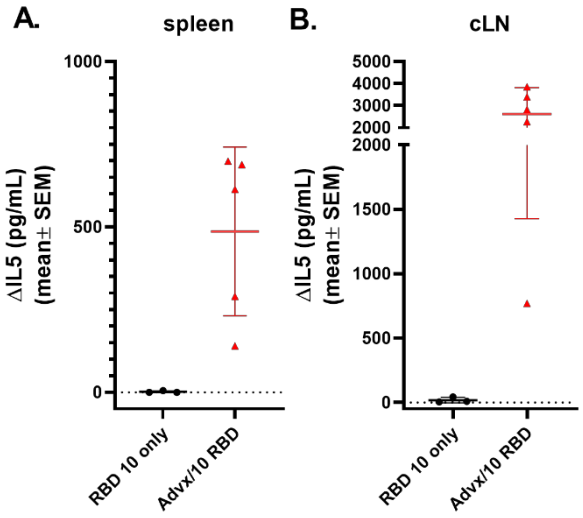

**Supplemental Figure S2.** Mucosal response assessed in immunized mice by measuring S1-specific IgA in bronchial alveolar lavage after prime/boost/boost immunizations (10 weeks post-initial immunization) as measured by ELISA. Absorbance values at 405 nm are shown after development with an alkaline-phosphatase conjugated secondary antibody with a pNPP substrate.

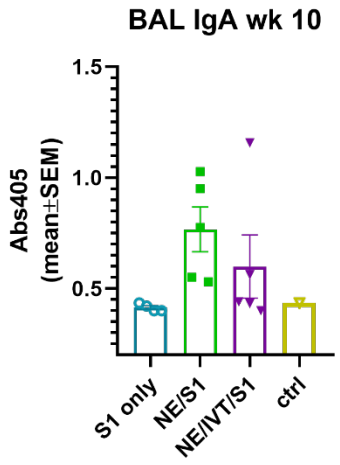

## References:


1. https://coronavirus.jhu.edu/map.html (accessed 02/15/20).
2. Thanh Le, T.; Andreadakis, Z.; Kumar, A.; Gómez Román, R.; Tollefsen, S.; Saville, M.; Mayhew, S., The COVID-19 vaccine development landscape. *Nature reviews. Drug discovery* **2020,** *19* (5), 305-306.
3. O'Callaghan, K. P.; Blatz, A. M.; Offit, P. A., Developing a SARS-CoV-2 Vaccine at Warp Speed. *Jama* **2020,** *324* (5), 437-438.
4. Corey, L.; Mascola, J. R.; Fauci, A. S.; Collins, F. S., A strategic approach to COVID-19 vaccine R&D. *Science* **2020,** *368* (6494), 948-950.
5. Mascola, J. R.; Graham, B. S.; Fauci, A. S., SARS-CoV-2 Viral Variants-Tackling a Moving Target. *Jama* **2021**.
6. Tegally, H.; Wilkinson, E.; Giovanetti, M.; Iranzadeh, A.; Fonseca, V.; Giandhari, J.; Doolabh, D.; Pillay, S.; San, E. J.; Msomi, N.; Mlisana, K.; von Gottberg, A.; Walaza, S.; Allam, M.; Ismail, A.; Mohale, T.; Glass, A. J.; Engelbrecht, S.; Van Zyl, G.; Preiser, W.; Petruccione, F.; Sigal, A.; Hardie, D.; Marais, G.; Hsiao, M.; Korsman, S.; Davies, M.-A.; Tyers, L.; Mudau, I.; York, D.; Maslo, C.; Goedhals, D.; Abrahams, S.; Laguda-Akingba, O.; Alisoltani-Dehkordi, A.; Godzik, A.; Wibmer, C. K.; Sewell, B. T.; Lourenço, J.; Alcantara, L. C. J.; Pond, S. L. K.; Weaver, S.; Martin, D.; Lessells, R. J.; Bhiman, J. N.; Williamson, C.; de Oliveira, T., Emergence and rapid spread of a new severe acute respiratory syndrome-related coronavirus 2 (SARS-CoV-2) lineage with multiple spike mutations in South Africa. **2020**, 2020.12.21.20248640.
7. Jangra, S.; Ye, C.; Rathnasinghe, R.; Stadlbauer, D.; Krammer, F.; Simon, V.; Martinez-Sobrido, L.; Garcia-Sastre, A.; Schotsaert, M., The E484K mutation in the SARS-CoV-2 spike protein reduces but does not abolish neutralizing activity of human convalescent and post-vaccination sera. *medRxiv* **2021**.
8. David, H.; Pengfei, W.; Lihong, L.; Sho, I.; Yang, L.; Yicheng, G.; Maple, W.; Jian, Y.; Baoshan, Z.; Peter, K.; Barney, G.; John, M.; Jennifer, C.; Michael, Y.; Magdalena, S.; Christos, K.; Lawrence, S.; Zizhang, S.; Manoj, N.; Yaoxing, H., Increased Resistance of SARS-CoV-2 Variants B.1.351 and B.1.1.7 to Antibody Neutralization. *Nature Portfolio* **2021**.
9. Johnson, J. Johnson & Johnson announces single-shot Janssen COVID-19 vaccine candidate met primary endpoints in interim analysis of its phase 3 ENSEMBLE trial. . https://www.jnj.com/johnson-johnson-announces-single-shot-janssen-covid-19-vaccine-candidate-met-primary-endpoints-in-interim-analysis-of-its-phase-3-ensemble-trial (accessed 02/14/2021).
10. Novavax Novavax COVID-19 vaccine demonstrates 89.3% efficacy in UK phase 3 trial. https://ir.novavax.com/news-releases/news-release-details/novavax-covid-19-vaccine-demonstrates-893-efficacy-uk-phase-3 (accessed 02/14/21).
11. Vabret, N.; Britton, G. J.; Gruber, C.; Hegde, S.; Kim, J.; Kuksin, M.; Levantovsky, R.; Malle, L.; Moreira, A.; Park, M. D.; Pia, L.; Risson, E.; Saffern, M.; Salomé, B.; Esai Selvan, M.; Spindler, M. P.; Tan, J.; van der Heide, V.; Gregory, J. K.; Alexandropoulos, K.; Bhardwaj, N.; Brown, B. D.; Greenbaum, B.; Gümüş, Z. H.; Homann, D.; Horowitz, A.; Kamphorst, A. O.; Curotto de Lafaille, M. A.; Mehandru, S.; Merad, M.; Samstein, R. M., Immunology of COVID-19: Current State of the Science. *Immunity* **2020,** *52* (6), 910-941.
12. Sette, A.; Crotty, S., Adaptive immunity to SARS-CoV-2 and COVID-19. *Cell* **2021**.
13. Rydyznski Moderbacher, C.; Ramirez, S. I.; Dan, J. M.; Grifoni, A.; Hastie, K. M.; Weiskopf, D.; Belanger, S.; Abbott, R. K.; Kim, C.; Choi, J.; Kato, Y.; Crotty, E. G.; Kim, C.; Rawlings, S. A.; Mateus, J.; Tse, L. P. V.; Frazier, A.; Baric, R.; Peters, B.; Greenbaum, J.; Ollmann Saphire, E.; Smith, D. M.; Sette, A.; Crotty, S., Antigen-Specific Adaptive Immunity to SARS-CoV-2 in Acute COVID-19 and Associations with Age and Disease Severity. *Cell* **2020,** *183* (4), 996-1012.e19.
14. McMahan, K.; Yu, J.; Mercado, N. B.; Loos, C.; Tostanoski, L. H.; Chandrashekar, A.; Liu, J.; Peter, L.; Atyeo, C.; Zhu, A.; Bondzie, E. A.; Dagotto, G.; Gebre, M. S.; Jacob-Dolan, C.; Li, Z.;

Nampanya, F.; Patel, S.; Pessaint, L.; Van Ry, A.; Blade, K.; Yalley-Ogunro, J.; Cabus, M.; Brown, R.; Cook, A.; Teow, E.; Andersen, H.; Lewis, M. G.; Lauffenburger, D. A.; Alter, G.; Barouch, D. H., Correlates of protection against SARS-CoV-2 in rhesus macaques. *Nature* **2020**.

15. Okba, N. M. A.; Müller, M. A.; Li, W.; Wang, C.; GeurtsvanKessel, C. H.; Corman, V. M.; Lamers, M. M.; Sikkema, R. S.; de Bruin, E.; Chandler, F. D.; Yazdanpanah, Y.; Le Hingrat, Q.; Descamps, D.; Houhou-Fidouh, N.; Reusken, C.; Bosch, B. J.; Drosten, C.; Koopmans, M. P. G.; Haagmans, B. L., Severe Acute Respiratory Syndrome Coronavirus 2-Specific Antibody Responses in Coronavirus Disease Patients. *Emerging infectious diseases* **2020,** *26* (7), 1478-1488.
16. Crotty, S., T Follicular Helper Cell Biology: A Decade of Discovery and Diseases. *Immunity* **2019,** *50* (5), 1132-1148.
17. Channappanavar, R.; Fett, C.; Zhao, J.; Meyerholz, D. K.; Perlman, S., Virus-specific memory CD8 T cells provide substantial protection from lethal severe acute respiratory syndrome coronavirus infection. *J Virol* **2014,** *88* (19), 11034-44.
18. Hogan, R. J.; Usherwood, E. J.; Zhong, W.; Roberts, A. A.; Dutton, R. W.; Harmsen, A. G.; Woodland, D. L., Activated antigen-specific CD8+ T cells persist in the lungs following recovery from respiratory virus infections. *Journal of immunology (Baltimore, Md. : 1950)* **2001,** *166* (3), 1813-22.
19. Slutter, B.; Pewe, L. L.; Kaech, S. M.; Harty, J. T., Lung airway-surveilling CXCR3(hi) memory CD8(+) T cells are critical for protection against influenza A virus. *Immunity* **2013,** *39* (5), 939-48.
20. Wu, T.; Hu, Y.; Lee, Y. T.; Bouchard, K. R.; Benechet, A.; Khanna, K.; Cauley, L. S., Lung-resident memory CD8 T cells (TRM) are indispensable for optimal cross-protection against pulmonary virus infection. *Journal of leukocyte biology* **2014,** *95* (2), 215-24.
21. Zhao, J.; Zhao, J.; Mangalam, A. K.; Channappanavar, R.; Fett, C.; Meyerholz, D. K.; Agnihothram, S.; Baric, R. S.; David, C. S.; Perlman, S., Airway Memory CD4(+) T Cells Mediate Protective Immunity against Emerging Respiratory Coronaviruses. *Immunity* **2016,** *44* (6), 1379-91.
22. Gorman, M. J.; Patel, N.; Guebre-Xabier, M.; Zhu, A.; Atyeo, C.; Pullen, K. M.; Loos, C.; Goez-Gazi, Y.; Carrion, R.; Tian, J. H.; Yaun, D.; Bowman, K.; Zhou, B.; Maciejewski, S.; McGrath, M. E.; Logue, J.; Frieman, M. B.; Montefiori, D.; Mann, C.; Schendel, S.; Amanat, F.; Krammer, F.; Saphire, E. O.; Lauffenburger, D.; Greene, A. M.; Portnoff, A. D.; Massare, M. J.; Ellingsworth, L.; Glenn, G.; Smith, G.; Alter, G., Collaboration between the Fab and Fc contribute to maximal protection against SARS-CoV-2 in nonhuman primates following NVX-CoV2373 subunit vaccine with Matrix-M™ vaccination. *bioRxiv* **2021**.
23. Callaway, E.; Mallapaty, S., Novavax offers first evidence that COVID vaccines protect people against variants. *Nature* **2021,** *590* (7844), 17.
24. Richmond, P.; Hatchuel, L.; Dong, M.; Ma, B.; Hu, B.; Smolenov, I.; Li, P.; Liang, P.; Han, H. H.; Liang, J.; Clemens, R., Safety and immunogenicity of S-Trimer (SCB-2019), a protein subunit vaccine candidate for COVID-19 in healthy adults: a phase 1, randomised, double-blind, placebo-controlled trial. *Lancet* **2021**.
25. Leroux-Roels, G., Prepandemic H5N1 influenza vaccine adjuvanted with AS03: a review of the pre-clinical and clinical data. *Expert Opin Biol Ther* **2009,** *9* (8), 1057-71.
26. Hamouda, T.; Sutcliffe, J. A.; Ciotti, S.; Baker, J. R., Jr., Intranasal immunization of ferrets with commercial trivalent influenza vaccines formulated in a nanoemulsion-based adjuvant. *Clin Vaccine Immunol* **2011,** *18* (7), 1167-75.
27. Seow, J.; Graham, C.; Merrick, B.; Acors, S.; Pickering, S.; Steel, K. J. A.; Hemmings, O.; O'Byrne, A.; Kouphou, N.; Galao, R. P.; Betancor, G.; Wilson, H. D.; Signell, A. W.; Winstone, H.; Kerridge, C.; Huettner, I.; Jimenez-Guardeño, J. M.; Lista, M. J.; Temperton, N.; Snell, L. B.; Bisnauthsing, K.; Moore, A.; Green, A.; Martinez, L.; Stokes, B.; Honey, J.; Izquierdo-Barras, A.; Arbane, G.; Patel, A.; Tan, M. K. I.; O'Connell, L.; O'Hara, G.; MacMahon, E.; Douthwaite, S.; Nebbia, G.; Batra, R.; Martinez-Nunez, R.; Shankar-Hari, M.; Edgeworth, J. D.; Neil, S. J. D.; Malim, M. H.; Doores, K. J., Longitudinal observation and decline of neutralizing antibody responses in the three months following SARS-CoV-2 infection in humans. *Nature microbiology* **2020,** *5* (12), 1598-1607.

28. Blanco-Melo, D.; Nilsson-Payant, B. E.; Liu, W. C.; Uhl, S.; Hoagland, D.; Moller, R.; Jordan, T. X.; Oishi, K.; Panis, M.; Sachs, D.; Wang, T. T.; Schwartz, R. E.; Lim, J. K.; Albrecht, R. A.; tenOever, B. R., Imbalanced Host Response to SARS-CoV-2 Drives Development of COVID-19. *Cell* **2020,** *181* (5), 1036-1045 e9.
29. Perry, A. K.; Chen, G.; Zheng, D.; Tang, H.; Cheng, G., The host type I interferon response to viral and bacterial infections. *Cell research* **2005,** *15* (6), 407-22.
30. Park, A.; Iwasaki, A., Type I and Type III Interferons - Induction, Signaling, Evasion, and Application to Combat COVID-19. *Cell Host Microbe* **2020,** *27* (6), 870-878.
31. Daffis, S.; Szretter, K. J.; Schriewer, J.; Li, J.; Youn, S.; Errett, J.; Lin, T. Y.; Schneller, S.; Zust, R.; Dong, H.; Thiel, V.; Sen, G. C.; Fensterl, V.; Klimstra, W. B.; Pierson, T. C.; Buller, R. M.; Gale, M., Jr.; Shi, P. Y.; Diamond, M. S., 2'-O methylation of the viral mRNA cap evades host restriction by IFIT family members. *Nature* **2010,** *468* (7322), 452-6.
32. Chen, Y.; Cai, H.; Pan, J.; Xiang, N.; Tien, P.; Ahola, T.; Guo, D., Functional screen reveals SARS coronavirus nonstructural protein nsp14 as a novel cap N7 methyltransferase. *Proceedings of the National Academy of Sciences of the United States of America* **2009,** *106* (9), 3484-9.
33. Iwata-Yoshikawa, N.; Uda, A.; Suzuki, T.; Tsunetsugu-Yokota, Y.; Sato, Y.; Morikawa, S.; Tashiro, M.; Sata, T.; Hasegawa, H.; Nagata, N., Effects of Toll-like receptor stimulation on eosinophilic infiltration in lungs of BALB/c mice immunized with UV-inactivated severe acute respiratory syndrome-related coronavirus vaccine. *J Virol* **2014,** *88* (15), 8597-614.
34. Stanberry, L. R.; Simon, J. K.; Johnson, C.; Robinson, P. L.; Morry, J.; Flack, M. R.; Gracon, S.; Myc, A.; Hamouda, T.; Baker, J. R., Jr., Safety and immunogenicity of a novel nanoemulsion mucosal adjuvant W805EC combined with approved seasonal influenza antigens. *Vaccine* **2012,** *30* (2), 307-16.
35. Safety and Immunogenicity Study of Inactivated Nasal Influenza Vaccine NB-1008 Administered by Sprayer. *ClinicalTrials.gov Identifier: NCT01354379* **Start date May 2011**.
36. A Safety and Immunogenicity of Intranasal Nanoemulsion Adjuvanted Recombinant Anthrax Vaccine in Healthy Adults (IN NE-rPA). *ClinicalTrials.gov Identifier: NCT04148118* **Start date January 8, 2020**.
37. Wong, P. T.; Wang, S. H.; Ciotti, S.; Makidon, P. E.; Smith, D. M.; Fan, Y.; Schuler, C. F. t.; Baker, J. R., Jr., Formulation and characterization of nanoemulsion intranasal adjuvants: effects of surfactant composition on mucoadhesion and immunogenicity. *Molecular pharmaceutics* **2014,** *11* (2), 531-44.
38. Wong, P. T.; Leroueil, P. R.; Smith, D. M.; Ciotti, S.; Bielinska, A. U.; Janczak, K. W.; Mullen, C. H.; Groom, J. V., 2nd; Taylor, E. M.; Passmore, C.; Makidon, P. E.; O'Konek, J. J.; Myc, A.; Hamouda, T.; Baker, J. R., Jr., Formulation, high throughput in vitro screening and in vivo functional characterization of nanoemulsion-based intranasal vaccine adjuvants. *Plos One* **2015,** *10* (5), e0126120.
39. Bielinska, A. U.; Makidon, P. E.; Janczak, K. W.; Blanco, L. P.; Swanson, B.; Smith, D. M.; Pham, T.; Szabo, Z.; Kukowska-Latallo, J. F.; Baker, J. R., Jr., Distinct pathways of humoral and cellular immunity induced with the mucosal administration of a nanoemulsion adjuvant. *Journal of immunology (Baltimore, Md. : 1950)* **2014,** *192* (6), 2722-33.
40. Bielinska, A. U.; Chepurnov, A. A.; Landers, J. J.; Janczak, K. W.; Chepurnova, T. S.; Luker, G. D.; Baker, J. R., Jr., A novel, killed-virus nasal vaccinia virus vaccine. *Clin Vaccine Immunol* **2008,** *15* (2), 348-58.
41. Bielinska, A. U.; Janczak, K. W.; Landers, J. J.; Makidon, P.; Sower, L. E.; Peterson, J. W.; Baker, J. R., Jr., Mucosal immunization with a novel nanoemulsion-based recombinant anthrax protective antigen vaccine protects against Bacillus anthracis spore challenge. *Infect Immun* **2007,** *75* (8), 4020-9.
42. Bielinska, A. U.; Janczak, K. W.; Landers, J. J.; Markovitz, D. M.; Montefiori, D. C.; Baker, J. R., Jr., Nasal immunization with a recombinant HIV gp120 and nanoemulsion adjuvant produces Th1 polarized responses and neutralizing antibodies to primary HIV type 1 isolates. *AIDS Res Hum Retroviruses* **2008,** *24* (2), 271-81.

43. Makidon, P. E.; Belyakov, I. M.; Blanco, L. P.; Janczak, K. W.; Landers, J.; Bielinska, A. U.; Groom, J. V., 2nd; Baker, J. R., Jr., Nanoemulsion mucosal adjuvant uniquely activates cytokine production by nasal ciliated epithelium and induces dendritic cell trafficking. *Eur J Immunol* **2012,** *42* (8), 2073-86.
44. Myc, A.; Kukowska-Latallo, J. F.; Smith, D. M.; Passmore, C.; Pham, T.; Wong, P.; Bielinska, A. U.; Baker, J. R., Jr., Nanoemulsion nasal adjuvant W(8)(0)5EC induces dendritic cell engulfment of antigen-primed epithelial cells. *Vaccine* **2013,** *31* (7), 1072-9.
45. Martinez-Gil, L.; Goff, P. H.; Hai, R.; Garcia-Sastre, A.; Shaw, M. L.; Palese, P., A Sendai virus-derived RNA agonist of RIG-I as a virus vaccine adjuvant. *J Virol* **2013,** *87* (3), 1290-300.
46. Patel, J. R.; Jain, A.; Chou, Y. Y.; Baum, A.; Ha, T.; Garcia-Sastre, A., ATPase-driven oligomerization of RIG-I on RNA allows optimal activation of type-I interferon. *EMBO reports* **2013,** *14* (9), 780-7.
47. Wong, P. T.; Goff, P. H.; Sun, R. J.; Ruge, M. J.; Ermler, M. E.; Sebring, A.; O'Konek, J. J.; Landers, J. J.; Janczak, K. W.; Sun, W.; Baker, J. R., Jr., Combined Intranasal Nanoemulsion and RIG-I Activating RNA Adjuvants Enhance Mucosal, Humoral, and Cellular Immunity to Influenza Virus. *Molecular pharmaceutics* **2020**.
48. Crawford, K. H. D.; Eguia, R.; Dingens, A. S.; Loes, A. N.; Malone, K. D.; Wolf, C. R.; Chu, H. Y.; Tortorici, M. A.; Veesler, D.; Murphy, M.; Pettie, D.; King, N. P.; Balazs, A. B.; Bloom, J. D., Protocol and Reagents for Pseudotyping Lentiviral Particles with SARS-CoV-2 Spike Protein for Neutralization Assays. *Viruses* **2020,** *12* (5).
49. Rathnasinghe, R.; Jangra, S.; Cupic, A.; Martínez-Romero, C.; Mulder, L. C. F.; Kehrer, T.; Yildiz, S.; Choi, A.; Mena, I.; De Vrieze, J.; Aslam, S.; Stadlbauer, D.; Meekins, D. A.; McDowell, C. D.; Balaraman, V.; Richt, J. A.; De Geest, B. G.; Miorin, L.; Krammer, F.; Simon, V.; García-Sastre, A.; Schotsaert, M., The N501Y mutation in SARS-CoV-2 spike leads to morbidity in obese and aged mice and is neutralized by convalescent and post-vaccination human sera. *medRxiv* **2021**.
50. Wang, S. H.; Chen, J.; Smith, D.; Cao, Z.; Acosta, H.; Fan, Y.; Ciotti, S.; Fattom, A.; Baker, J., Jr., A novel combination of intramuscular vaccine adjuvants, nanoemulsion and CpG produces an effective immune response against influenza A virus. *Vaccine* **2020,** *38* (19), 3537-3544.
51. Wang, S. H.; Smith, D.; Cao, Z.; Chen, J.; Acosta, H.; Chichester, J. A.; Yusibov, V.; Streatfield, S. J.; Fattom, A.; Baker, J. R., Jr., Recombinant H5 hemagglutinin adjuvanted with nanoemulsion protects ferrets against pathogenic avian influenza virus challenge. *Vaccine* **2019,** *37* (12), 1591-1600.
52. O'Konek, J. J.; Makidon, P. E.; Landers, J. J.; Cao, Z.; Malinczak, C. A.; Pannu, J.; Sun, J.; Bitko, V.; Ciotti, S.; Hamouda, T.; Wojcinski, Z. W.; Lukacs, N. W.; Fattom, A.; Baker, J. R., Jr., Intranasal nanoemulsion-based inactivated respiratory syncytial virus vaccines protect against viral challenge in cotton rats. *Human vaccines & immunotherapeutics* **2015,** *11* (12), 2904-12.
53. Li, J.; Ulitzky, L.; Silberstein, E.; Taylor, D. R.; Viscidi, R., Immunogenicity and protection efficacy of monomeric and trimeric recombinant SARS coronavirus spike protein subunit vaccine candidates. *Viral Immunol* **2013,** *26* (2), 126-32.
54. Amanat, F.; Strohmeier, S.; Rathnasinghe, R.; Schotsaert, M.; Coughlan, L.; García-Sastre, A.; Krammer, F., Introduction of two prolines and removal of the polybasic cleavage site leads to optimal efficacy of a recombinant spike based SARS-CoV-2 vaccine in the mouse model. *bioRxiv* **2020**.
55. Wang, Y.; Wang, L.; Cao, H.; Liu, C., SARS-CoV-2 S1 is superior to the RBD as a COVID-19 subunit vaccine antigen. *Journal of medical virology* **2021,** *93* (2), 892-898.
56. Zhang, J.; Wu, Q.; Liu, Z.; Wang, Q.; Wu, J.; Hu, Y.; Bai, T.; Xie, T.; Huang, M.; Wu, T.; Peng, D.; Huang, W.; Jin, K.; Niu, L.; Guo, W.; Luo, D.; Lei, D.; Wu, Z.; Li, G.; Huang, R.; Lin, Y.; Xie, X.; He, S.; Deng, Y.; Liu, J.; Li, W.; Lu, Z.; Chen, H.; Zeng, T.; Luo, Q.; Li, Y. P.; Wang, Y.; Liu, W.; Qu, X., Spike-specific circulating T follicular helper cell and cross-neutralizing antibody responses in COVID-19-convalescent individuals. *Nature microbiology* **2021,** *6* (1), 51-58.

57. Bielinska, A. U.; Gerber, M.; Blanco, L. P.; Makidon, P. E.; Janczak, K. W.; Beer, M.; Swanson, B.; Baker, J. R., Jr., Induction of Th17 cellular immunity with a novel nanoemulsion adjuvant. *Crit Rev Immunol* **2010,** *30* (2), 189-99.
58. Passmore, C.; Makidon, P. E.; O'Konek, J. J.; Zahn, J. A.; Pannu, J.; Hamouda, T.; Bitko, V.; Myc, A.; Lukacs, N. W.; Fattom, A.; Baker, J. R., Jr., Intranasal immunization with W 80 5EC adjuvanted recombinant RSV rF-ptn enhances clearance of respiratory syncytial virus in a mouse model. *Human vaccines & immunotherapeutics* **2014,** *10* (3), 615-22.
59. Ou, X.; Liu, Y.; Lei, X.; Li, P.; Mi, D.; Ren, L.; Guo, L.; Guo, R.; Chen, T.; Hu, J.; Xiang, Z.; Mu, Z.; Chen, X.; Chen, J.; Hu, K.; Jin, Q.; Wang, J.; Qian, Z., Characterization of spike glycoprotein of SARS-CoV-2 on virus entry and its immune cross-reactivity with SARS-CoV. *Nat Commun* **2020,** *11* (1), 1620.
60. Dan, J. M.; Mateus, J.; Kato, Y.; Hastie, K. M.; Yu, E. D.; Faliti, C. E.; Grifoni, A.; Ramirez, S. I.; Haupt, S.; Frazier, A.; Nakao, C.; Rayaprolu, V.; Rawlings, S. A.; Peters, B.; Krammer, F.; Simon, V.; Saphire, E. O.; Smith, D. M.; Weiskopf, D.; Sette, A.; Crotty, S., Immunological memory to SARS-CoV-2 assessed for up to 8 months after infection. *Science* **2021,** *371* (6529).
61. Sahin, U.; Muik, A.; Vogler, I.; Derhovanessian, E.; Kranz, L. M.; Vormehr, M.; Quandt, J.; Bidmon, N.; Ulges, A.; Baum, A.; Pascal, K.; Maurus, D.; Brachtendorf, S.; Lörks, V.; Sikorski, J.; Koch, P.; Hilker, R.; Becker, D.; Eller, A.-K.; Grützner, J.; Tonigold, M.; Boesler, C.; Rosenbaum, C.; Heesen, L.; Kühnle, M.-C.; Poran, A.; Dong, J. Z.; Luxemburger, U.; Kemmer-Brück, A.; Langer, D.; Bexon, M.; Bolte, S.; Palanche, T.; Schultz, A.; Baumann, S.; Mahiny, A. J.; Boros, G.; Reinholz, J.; Szabó, G. T.; Karikó, K.; Shi, P.-Y.; Fontes-Garfias, C.; Perez, J. L.; Cutler, M.; Cooper, D.; Kyratsous, C. A.; Dormitzer, P. R.; Jansen, K. U.; Türeci, Ö., BNT162b2 induces SARS-CoV-2-neutralising antibodies and T cells in humans. **2020**, 2020.12.09.20245175.
62. Corbett, K. S.; Edwards, D. K.; Leist, S. R.; Abiona, O. M.; Boyoglu-Barnum, S.; Gillespie, R. A.; Himansu, S.; Schäfer, A.; Ziwawo, C. T.; DiPiazza, A. T.; Dinnon, K. H.; Elbashir, S. M.; Shaw, C. A.; Woods, A.; Fritch, E. J.; Martinez, D. R.; Bock, K. W.; Minai, M.; Nagata, B. M.; Hutchinson, G. B.; Wu, K.; Henry, C.; Bahl, K.; Garcia-Dominguez, D.; Ma, L.; Renzi, I.; Kong, W. P.; Schmidt, S. D.; Wang, L.; Zhang, Y.; Phung, E.; Chang, L. A.; Loomis, R. J.; Altaras, N. E.; Narayanan, E.; Metkar, M.; Presnyak, V.; Liu, C.; Louder, M. K.; Shi, W.; Leung, K.; Yang, E. S.; West, A.; Gully, K. L.; Stevens, L. J.; Wang, N.; Wrapp, D.; Doria-Rose, N. A.; Stewart-Jones, G.; Bennett, H.; Alvarado, G. S.; Nason, M. C.; Ruckwardt, T. J.; McLellan, J. S.; Denison, M. R.; Chappell, J. D.; Moore, I. N.; Morabito, K. M.; Mascola, J. R.; Baric, R. S.; Carfi, A.; Graham, B. S., SARS-CoV-2 mRNA vaccine design enabled by prototype pathogen preparedness. *Nature* **2020,** *586* (7830), 567-571.
63. Coffman, R. L.; Sher, A.; Seder, R. A., Vaccine adjuvants: putting innate immunity to work. *Immunity* **2010,** *33* (4), 492-503.
64. Seder, R. A.; Darrah, P. A.; Roederer, M., T-cell quality in memory and protection: implications for vaccine design. *Nat Rev Immunol* **2008,** *8* (4), 247-58.
65. Jangra, S.; De Vrieze, J.; Choi, A.; Rathnasinghe, R.; Laghlali, G.; Uvyn, A.; Van Herck, S.; Nuhn, L.; Deswarte, K.; Zhong, Z.; Sanders, N.; Lienenklaus, S.; David, S.; Strohmeier, S.; Amanat, F.; Krammer, F.; Hammad, H.; Lambrecht, B. N.; Coughlan, L.; García-Sastre, A.; de Geest, B.; Schotsaert, M., Sterilizing Immunity against SARS-CoV-2 Infection in Mice by a Single-Shot and Lipid Amphiphile Imidazoquinoline TLR7/8 Agonist-Adjuvanted Recombinant Spike Protein Vaccine. *Angewandte Chemie (International ed. in English)* **2021**.
66. Bolles, M.; Deming, D.; Long, K.; Agnihothram, S.; Whitmore, A.; Ferris, M.; Funkhouser, W.; Gralinski, L.; Totura, A.; Heise, M.; Baric, R. S., A double-inactivated severe acute respiratory syndrome coronavirus vaccine provides incomplete protection in mice and induces increased eosinophilic proinflammatory pulmonary response upon challenge. *J Virol* **2011,** *85* (23), 12201-15.
67. Honda-Okubo, Y.; Barnard, D.; Ong, C. H.; Peng, B. H.; Tseng, C. T.; Petrovsky, N., Severe acute respiratory syndrome-associated coronavirus vaccines formulated with delta inulin adjuvants provide

enhanced protection while ameliorating lung eosinophilic immunopathology. *J Virol* **2015,** *89* (6), 2995-3007.

68. Dubin, P. J.; Kolls, J. K., Th17 cytokines and mucosal immunity. *Immunol Rev* **2008,** *226*, 160-71.
69. Christensen, D.; Mortensen, R.; Rosenkrands, I.; Dietrich, J.; Andersen, P., Vaccine-induced Th17 cells are established as resident memory cells in the lung and promote local IgA responses. *Mucosal Immunol* **2017,** *10* (1), 260-270.
70. Gauttier, V.; Morello, A.; Girault, I.; Mary, C.; Belarif, L.; Desselle, A.; Wilhelm, E.; Bourquard, T.; Pengam, S.; Teppaz, G.; Thepenier, V.; Biteau, K.; De Barbeyrac, E.; Kiepferlé, D.; Vasseur, B.; Le Flem, F.; Debieuvre, D.; Costantini, D.; Poirier, N., Tissue-resident memory CD8 T-cell responses elicited by a single injection of a multi-target COVID-19 vaccine. **2020**, 2020.08.14.240093.
71. Xu, S.; Cao, X., Interleukin-17 and its expanding biological functions. *Cell Mol Immunol* **2010,** *7* (3), 164-74.
72. Lindell, D. M.; Morris, S. B.; White, M. P.; Kallal, L. E.; Lundy, P. K.; Hamouda, T.; Baker, J. R., Jr.; Lukacs, N. W., A novel inactivated intranasal respiratory syncytial virus vaccine promotes viral clearance without Th2 associated vaccine-enhanced disease. *Plos One* **2011,** *6* (7), e21823.
73. Son, Y. M.; Cheon, I. S.; Wu, Y.; Li, C.; Wang, Z.; Gao, X.; Chen, Y.; Takahashi, Y.; Fu, Y. X.; Dent, A. L.; Kaplan, M. H.; Taylor, J. J.; Cui, W.; Sun, J., Tissue-resident CD4(+) T helper cells assist the development of protective respiratory B and CD8(+) T cell memory responses. *Sci Immunol* **2021,** *6* (55).